and Ki-67 has been reported (Nam et al., 2008; Queiroz et al., 2006), accumulation of $p16^{INK4a}$ was not detected in the Ki-67 positive cells (data not shown) in the present case whose clinical behavior and histopathological findings were benign (Kawai et al., 2009).

In conclusion, HPV 126, isolated and characterized in the present study, is a novel type of genus gamma papillomavirus and associated with flat wart- or EV-related tinea versicolor-like clinical features: histological ICBs as with other genus gamma papillomaviruses; and immunohistochemical expression of Ki-67 and p53 in characteristic manner not typical for benign cutaneous warts. It is probable that conditions accompanying immunosuppression in this ATL patient may have contributed to stimulate viral production of HPV 126, thus leading to wart formation, as known for acquired EV (Lutzner et al., 1983). To ascertain the true nature of HPV 126 and its associated warts, we need to perform epidemiological as well as further clinicopathological and virological studies on a larger number of lesions and patients, including immunocompromised individuals.

Materials and methods

Patient

A 56-year-old Japanese man was referred to us in August 2008 for evaluation of a 5-year history of disseminated hypopigmented macules clinically resembling flat warts or epidermodysplasia verruciformis-related tinea versicolor-like lesions (Jablonska and Orth, 1985) on the chest, neck, and extremities (Fig. 1A) (Kawai et al., 2009). The patient might have been suffering from immunodeficiency, because he was diagnosed as having chronic type of adult T-cell leukemia at the age of 52 years and manifested recurrent fungal pneumonia, rapidly progressing oral squamous cell carcinoma and multiple brain abscesses. A biopsy specimen was taken from the flat wart-like lesions with adjacent normal skin under suspicion of acquired EV (Lutzner et al., 1983). The biopsy specimen was cut into two pieces, one of which was fixed in 20% buffered formalin and embedded in paraffin for conventional histopathological and immunohistochemical analyses, and the other was frozen and stored in −70 °C for further analyses including DNA extraction.

Microscopical examination

Four-micrometer thick sections were obtained from the formalin-fixed and paraffin-embedded biopsy specimen, stained with hematoxylin and eosin (H&E), and examined microscopically.

Cloning and characterization of HPV DNA

Degenerate primers to detect genus gamma papillomaviruses were as described previously (Kawai et al., 2009). The amplified sequence turned out to correspond to nt 4641 to 5632 of the cloned HPV126 (Supplementary Fig. 1). Then abutting primers were designed juxtaposing the *Hpa*I site present in the L1 region (forward primer: 5′-GTTAACAGTAGGCCATCCCTATTTTGATATTGTTG-3′, reverse primer: 5′-GTTAACAGTCTTTCAGTATTTGCATGAAAATAAATATCG-3′). The genome was amplified by 30 cycles of PCR using KOD plus DNA polymerase (Toyobo, Japan) according to the supplier's instruction; annealing at 60 °C, elongation at 68 °C for 8 min. About 8 kbp PCR products were purified and then cloned into pBluescriptIISK(−) (Stratagene, La Jolla, CA), in which 15-bp overlapping sequence of HPV 126 was added to the *Not*I site by PCR (forward primer: 5′-TGAAAGACTGTTAACGCGG-CCGCTCTAGAACTAGTGGATC-3′, reverse primer: 5′-TGGCCTACTGT-TAACGCGGCCGCCACCGCGGTGGAGCTCC-3′), by In-Fusion reaction (Clontech, Mountain View, CA). The complete genomic sequence of a clone was initially determined using primer walking by Nihon Gene Research Laboratories Inc. With the same set of primers (Supplementary Table 1), we confirmed the sequence of another clone from an independent PCR reaction to be identical (Supplementary Fig. 1). The DNA clone was submitted to the Human Papillomavirus Reference Laboratory (Heidelberg, Germany) for official designation, HPV 126, and the sequence was reconfirmed. HPV 126 sequence was submitted to DNA Data Bank of Japan (DDBJ) under accession number AB646346. Nucleotide sequence pairwise comparison of HPV 126 ORFs with types representing genus gamma papillomaviruses and L1 nucleotide global multiple sequence alignments were analyzed using ClustalW program (Thompson et al., 1994). Each gap was included and counted as one position. Phylogenetic analyses were conducted using MEGA version 4 (Tamura et al., 2007).

Immunohistochemical examination

Formalin-fixed and paraffin-embedded tissue sections (4 μm-thick) were deparaffinized in xylene and rehydrated through a series of graded ethanols (100–70%). For antigen retrieval, slides were immersed in citrate buffer (pH6.0) and were heated for 20 min in a microwave. The slides were then incubated in methanol containing 0.3% H_2O_2 to inhibit endogenous peroxidase activity. After washing, primary antibodies (Anti-papillomavirus common antigen, DAKO, clone K1H8, 1:200; Ki-67, DAKO, Clone MIB-1, 1:50; p53 protein, DAKO, Clone DO-7, 1:50; $p16^{INK4a}$, Santa Cruz, Clone JC8, 1:200; cytokeratin, Nichirei, polyclonal,1:2) were applied for 1 h and binding was detected using an Envision Kit (Dako Cytomation; K4006). Color development was achieved with 3, 3-diaminobenzine (DAB) as the chromogen and hematoxylin counterstaining was performed to aid in orientation. As a negative control, normal non-immune serum from the same source as the primary antibody was applied. Formalin-fixed, paraffin-embedded sections from an invasive uterine cervix squamous cell carcinoma biopsy served as a positive control for $p16^{INK4a}$.

Supplementary materials related to this article can be found online at doi: 10.1016/j.virol.2011.10.011.

Acknowledgments

Assignment of the HPV type number was kindly performed by Ethel-Michele de Villers, Human Papillomavirus Reference Laboratory, DKFZ, Heidelberg, Germany. We would like to express our appreciation to Takashi Yugawa, Tomomi Nakahara, and Shin-ichi Ohno for helpful discussions.

References

Bates, S., Phillips, A.C., Clark, P.A., Stott, F., Peters, G., Ludwig, R.L., Vousden, K.H., 1998. p14ARF links the tumour suppressors RB and p53. Nature 395, 124–125.

Bernard, H.U., Burk, R.D., Chen, Z., van Doorslaer, K., Hausen, H., de Villiers, E.M., 2010. Classification of papillomaviruses (PVs) based on 189 PV types and proposal of taxonomic amendments. Virology 401, 70–79.

de Villiers, E.M., Fauquet, C., Broker, T.R., Bernard, H.U., zur Hausen, H., 2004. Classification of papillomaviruses. Virology 324, 17–27.

Doorbar, J., Coneron, I., Gallimore, P.H., 1989. Sequence divergence yet conserved physical characteristics among the E4 proteins of cutaneous human papillomaviruses. Virology 172, 51–62.

Egawa, K., 1988. Another viral inclusion wart different from myrmecia. Nippon Hifuka Gakkai Zasshi 98, 1105–1112.

Egawa, K., 1994. New types of human papillomaviruses and intracytoplasmic inclusion bodies: a classification of inclusion warts according to clinical features, histology and associated HPV types. Br. J. Dermatol. 130, 158–166.

Egawa, K., 2005. Histochemical analysis of cutaneous HPV-associated lesions. Methods Mol. Med. 119, 27–40.

Egawa, K., 2007. Genus gamma- and mu-papillomaviruses: clinical and histopathological aspects suggestive of their important roles in virology and human pathology. Current Topics in Virology 6, 53–66.

Egawa, K., Delius, H., Matsukura, T., Kawashima, M., de Villiers, E.M., 1993. Two novel types of human papillomavirus, HPV 63 and HPV 65: comparisons of their clinical and histological features and DNA sequences to other HPV types. Virology 194, 789–799.

Forslund, O., Antonsson, A., Nordin, P., Stenquist, B., Hansson, B.G., 1999. A broad range of human papillomavirus types detected with a general PCR method suitable for analysis of cutaneous tumours and normal skin. J. Gen. Virol. 80 (Pt 9), 2437–2443.

Hiraiwa, A., Kiyono, T., Suzuki, S., Ohashi, M., Ishibashi, M., 1996. E7 proteins of four groups of human papillomaviruses, irrespective of their tissue tropism or cancer

association, possess the ability to transactivate transcriptional promoters E2F site dependently. Virus Genes 12, 27–35.
Honda, A., Iwasaki, T., Sata, T., Kawashima, M., Morishima, T., Matsukura, T., 1994. Human papillomavirus type 60-associated plantar wart. Ridged wart. Arch Dermatol 130, 1413–1417.
Jablonska, S., Orth, G., 1985. Epidermodysplasia verruciformis. Clin. Dermatol. 3, 83–96.
Jablonska, S., Orth, G., Obalek, S., Croissant, O., 1985. Cutaneous warts. Clinical, histologic, and virologic correlations. Clin. Dermatol. 3, 71–82.
Kawai, K., Egawa, N., Kiyono, T., Kanekura, T., 2009. Epidermodysplasia-verruciformis-like eruption associated with gamma-papillomavirus infection in a patient with adult T-cell leukemia. Dermatology 219, 274–278.
Li, L., Barry, P., Yeh, E., Glaser, C., Schnurr, D., Delwart, E., 2009. Identification of a novel human gammapapillomavirus species. J. Gen. Virol. 90, 2413–2417.
Lutzner, M.A., Orth, G., Dutronquay, V., Ducasse, M.F., Kreis, H., Crosnier, J., 1983. Detection of human papillomavirus type 5 DNA in skin cancers of an immunosuppressed renal allograft recipient. Lancet 2, 422–424.
Nam, E.J., Kim, J.W., Hong, J.W., Jang, H.S., Lee, S.Y., Jang, S.Y., Lee, D.W., Kim, S.W., Kim, J.H., Kim, Y.T., Kim, S., 2008. Expression of the p16 and Ki-67 in relation to the grade of cervical intraepithelial neoplasia and high-risk human papillomavirus infection. J Gynecol Oncol 19, 162–168.
Queiroz, C., Silva, T.C., Alves, V.A., Villa, L.L., Costa, M.C., Travassos, A.G., Filho, J.B., Studart, E., Cheto, T., de Freitas, L.A., 2006. Comparative study of the expression of cellular cycle proteins in cervical intraepithelial lesions. Pathol. Res. Pract. 202, 731–737.
Schmitt, A., Harry, J.B., Rapp, B., Wettstein, F.O., Iftner, T., 1994. Comparison of the properties of the E6 and E7 genes of low- and high-risk cutaneous papillomaviruses reveals strongly transforming and high Rb-binding activity for the E7 protein of the low-risk human papillomavirus type 1. J. Virol. 68, 7051–7059.
Tamura, K., Dudley, J., Nei, M., Kumar, S., 2007. MEGA4: Molecular Evolutionary Genetics Analysis (MEGA) software version 4.0. Mol. Biol. Evol. 24, 1596–1599.
Thompson, J.D., Higgins, D.G., Gibson, T.J., 1994. CLUSTAL W: improving the sensitivity of progressive multiple sequence alignment through sequence weighting, position-specific gap penalties and weight matrix choice. Nucleic Acids Res. 22, 4673–4680.

JVI
Journals.ASM.org

The E1 Protein of Human Papillomavirus Type 16 Is Dispensable for Maintenance Replication of the Viral Genome

Nagayasu Egawa,[a] Tomomi Nakahara,[a] Shin-ichi Ohno,[a] Mako Narisawa-Saito,[a] Takashi Yugawa,[a] Masatoshi Fujita,[a,b] Kenji Yamato,[c] Yukikazu Natori,[d] and Tohru Kiyono[a]

Division of Virology, National Cancer Center Research Institute, Tsukiji, Chuo-ku, Tokyo, Japan[a]; Department of Cellular Biochemistry, Graduate School of Pharmaceutical Sciences, Kyushu University, Maidashi, Higashi-ku, Fukuoka, Japan[b]; Section of Bacterial Pathogenesis, Tokyo Medical and Dental University, Graduate School of Medical and Dental Science, Yushima, Bunkyo-ku, Tokyo, Japan[c]; and RNAi Company Ltd., Hongo, Bunkyo-ku, Tokyo, Japan[d]

Papillomavirus genomes are thought to be amplified to about 100 copies per cell soon after infection, maintained constant at this level in basal cells, and amplified for viral production upon keratinocyte differentiation. To determine the requirement for E1 in viral DNA replication at different stages, an E1-defective mutant of the human papillomavirus 16 (HPV16) genome featuring a translation termination mutation in the E1 gene was used. The ability of the mutant HPV16 genome to replicate as nuclear episomes was monitored with or without exogenous expression of E1. Unlike the wild-type genome, the E1-defective HPV16 genome became established in human keratinocytes only as episomes in the presence of exogenous E1 expression. Once established, it could replicate with the same efficiency as the wild-type genome, even after the exogenous E1 was removed. However, upon calcium-induced keratinocyte differentiation, once again amplification was dependent on exogenous E1. These results demonstrate that the E1 protein is dispensable for maintenance replication but not for initial and productive replication of HPV16.

Papillomaviruses (PVs) are small, double-stranded DNA viruses that infect stratified squamous epithelium. Human PVs (HPVs) are very important causative agents for various lesions, ranging from verrucas to cancer. Among them, a subset of HPVs, the so-called high-risk types such as type 16 and 18, are associated with more than 90% of all cervical carcinomas as primary etiological factors (45). PVs establish long-term persistent infections in squamous epithelium, and the viral life cycle is tightly linked with the differentiation state of the host keratinocytes (7).

PV genome is replicated and amplified in three different stages: establishment, maintenance, and productive stages of the life cycle. In the establishment stage, soon after infection of the basal layer keratinocytes, a single or a few initial copies of the viral genome amplify and establish residence as multicopy circular extrachromosomal elements (episomes) in the nucleus. In the maintenance stage, the viral genomes in each affected cell replicate approximately once in a cell cycle in proliferating basal layer keratinocytes. Then, in the productive stage, they are exponentially amplified in terminally differentiating keratinocytes and packaged into progeny virions. It is important to understand the molecular mechanisms underlying this triphasic model for development of new therapies against HPV-infected lesions, such as cervical intraepithelial neoplasias, which can progress to cervical cancer.

The regulation of viral DNA replication is thought to differ in these three distinct stages of the viral life cycle. Studies of lesions experimentally induced by rabbit oral papillomavirus (ROPV) infection showed that the genome copy number of ROPV is low in the basal layer and increases up to four orders of magnitude during the terminal differentiation of host keratinocytes (21). This corresponds to more than 13 rounds of continuous replication of the viral genome in the productive stage.

Most of our knowledge of PV replication is derived from short-term replication assays to identify the components required for replication of the viral genome. These transient replication assays suggest that both viral proteins E1, a DNA helicase, and E2, a transcriptional activator and auxiliary replication factor, as well as *cis*-acting elements, including the E1-binding site (E1BS), several E2-binding sites (E2BS), and an AT-rich region in the long control region (LCR), are all essential for efficient PV DNA replication (4, 6, 20, 23, 30, 35, 37, 38). These studies appear to have analyzed the molecular mechanisms of viral replication in the productive stage, though they did not necessarily examine the three stages separately.

In this context, it is of interest that the HPV genome lacking LCR can replicate in the absence of both E1 and E2 proteins in transient replication assays (1, 16, 29), and a temperature-sensitive (TS) E1 mutant of bovine papillomavirus type 1 (BPV1) can be maintained in mouse C127 cells at a nonpermissive temperature as efficiently as the wild-type BPV1 (17). These reports suggest that E1 might be dispensable for maintenance replication.

To test this hypothesis directly, we here used an E1-defective mutant HPV16 genome featuring a translation termination mutation in E1. We established human dermal keratinocytes (HDKs) containing the E1-defective HPV16 genome with the help of exogenous E1 expression and then removed the exogenous E1 expression cassette with the FLP/FRT system (36). Similar to the wild-type genome, the E1-defective HPV16 genome was maintained for numerous cell generations without exogenous E1 expression. However, unlike the wild-type genomes, the E1-defective HPV16 genome failed to amplify upon differentiation of host cells, with rescue dependent on reexpression of exogenous E1. These results indicate that HPV16 requires E1 protein for the

Received 1 October 2011 Accepted 3 January 2012
Published ahead of print 11 January 2012
Address correspondence to Tohru Kiyono, tkiyono@ncc.go.jp.

doi:10.1128/JVI.06450-11

TABLE 1 Primers for PCR and RT-PCR

Name	nt position	Sequence (5′→3′)	Product size
For detecting excision of HPV16 DNA[a]			
For total HPV DNA, HPV16 E7	660	GGAGGAGGATGAAATAGATGGTC	136
	795	AGTACGAATGTCTACGTGTGTGC	
For excised-circular HPV DNA, HPV16 LCR	7432	AGGCCCATTTTGTAGCTTC	271
	7702	CCTAACAGCGGTATGTAAGG (+loxP 305)	
For detecting mRNAs			
HA-E1	7	CCTTATGACGTGCCAGATTACGC	144
	150	GTCATTTTCGTTCTCATCGTCTGAGATG	
E1^E4	603	TTTGCAACCAGAGACAACTGAT	933
	4014	AGAGGCTGCTGTTATCCACAAT	
36B4[b]	655	TCGACAATGGCAGCATCTAC	223
	877	GCCTTGACCTTTTCAGCAAG	
For real-time quantitative PCR to quantify HPV16 DNA			
HPV16 L2	4474	CCCACAGCTACAGATACACTTGCT	143
	4616	GGAATGGAAGGTACAGATGTTGGTGC	

[a] GenBank accession number for HPV16 is K02718.
[b] GenBank accession number for 36B4 is M17885.

establishment and the productive stages but not for the maintenance stage of viral genome replication. The results have important implications for the development of E1 inhibitors as anti-HPV drugs.

MATERIALS AND METHODS

Cell culture. Human dermal keratinocytes (HDKs) were purchased from Cell Applications (San Diego, CA). HDKs were immortalized with TERT, a mutant form of CDK4 and cyclin D1 (HDK-K4DT) by lentivirus-mediated gene transfer as described below. The cells were maintained in low-calcium serum-free keratinocyte growth medium (Epilife, Invitrogen, Carlsbad, CA) unless otherwise described. To induce keratinocyte differentiation, cells were exposed to Epilife basal medium supplemented with 1.8 mM $CaCl_2$ for 7 days or more. W12 (20863) cells were obtained from Paul F. Lambert (McArdle Laboratory for Cancer Research, Madison, WI) and cultured on mitomycin-treated Swiss mouse 3T3 cells in F medium as previously described (13).

Plasmid construction. In pCMV-loxP-HPV16-loxP-puro, the full-length HPV16 genome linearized at the SphI site in the long control region and flanked by *loxP* recombination sites (18) was inserted between a CMV promoter and a puromycin resistance gene so that the HPV16 genome was located in reverse orientation to the CMV promoter to avoid CMV-driven expression of HPV16 genes. In pCMV-loxP-E1-defective HPV16-loxP-puro, an in-frame stop codon was created at nucleotides (nt) 892 to 894 just downstream of the E1 start codon at nucleotide 865 by site-directed mutagenesis. The segment encoding Cre recombinase with nuclear localization signal in AxCANCre (14) was cloned into pcDNA3 (Invitrogen) to generate pcDNA3-NCre. Detailed methods for the construction of pCMV-loxP-HPV16-loxP-puro, pCMV-loxP-E1-defective-HPV16-loxP-puro, and pcDNA3-NCre are available upon request.

DNA transfection. HDK-K4DT cells were seeded at a density of 2×10^5 cells onto six-well plates (BD Biosciences, Franklin Lakes, NJ) containing 2 ml of Epilife and incubated overnight and then cotransfected with 1 μg of pcDNA3-NCre and 3 μg of pCMV-loxP-HPV16-loxP-puro (wild-type or E1-defective strains) using FuGENE HD (Roche). One day after transfection, cells were selected by 1 μg/ml of puromycin for 2 days.

Vector construction and retroviral infection. Construction of lentiviral vectors, CSII-CMV-TERT, CSII-CMV-cyclin D1, and CSII-CMV-$CDK4^{R24C}$, were described previously (33). CSII-CMV-TetON-ADV contains the TetON-ADV segment from pTet-On Advanced Vector (Clontech, Mountain View, CA). To yield improved E1 gene expression in mammalian cells, the codon-optimized HPV16 E1 gene with an N-terminal hemagglutinin (HA) tag (HA16E1) was synthesized (GenScript, Piscataway, NJ). CSII-TRE-Tight-HA16E1 contains the HA16E1 gene under the control of the tetracycline responsive promoter from pTRE-Tight (Clonetech). pCMSCV-FRT-HA-E1-TKneo consists of the CMV/LTR fusion promoter, the Ψ packaging signal, a mutant (f72) FLP recognition target (5′FRT) (24), the HA16E1 gene, the PKG promoter, and the herpes simplex virus thymidine kinase (HSV-TK) fused to the neomycin-resistant gene (*neo*), 3′FRT, and 3′LTR, as shown in Fig. 3A. Cells infected with this retrovirus were positively or negatively selected in the presence of 50 μg/ml of G418 or 10 μg/ml of ganciclovir, respectively. The nucleotide sequence of the HA16E1 and the detailed methods for the construction of pCMSCV-FRT-HA16E1-TKneo-FRT, CSII-CMV-TetON-ADV, and CSII-TRE-Tight-HA16E1 are available upon request. The production of recombinant retroviruses and lentiviruses was accomplished as described previously (27, 33).

AdV. The thermostable FLP mutant (FLPe)-expressing adenovirus vector (AdV) (AxCAFLPe), a kind gift from Izumi Saito (The Institute of Medical Science, The University of Tokyo), was prepared as described previously (3, 36). Cells were infected with AxCAFLPe at a 5-particle titer multiplicity of infection.

Western analysis. Western blotting was conducted as described previously (26). Antibodies against HA (16B12; Covance, Princeton, NJ), involucrin (SY5; Sigma-Aldrich, St. Louis, MO), vinculin (Sigma-Aldrich), and loricrin (Covance) were used as probes, and horseradish peroxidase-conjugated anti-mouse, anti-rabbit (Jackson ImmunoResearch Laboratories, West Grove, PA), or anti-goat (sc-2033; Santa Cruz, Santa Cruz, CA) immunoglobulins were employed as secondary antibodies.

PCR and DNA blot hybridization. Total genomic DNA was isolated by a standard SDS-proteinase K method, and an aliquot (100 ng) was examined by PCR amplification for Cre-mediated HPV DNA excision. Primer sets used for detecting total HPV16 DNA or recombined HPV16 are shown in Table 1. The DNA was amplified by 30 cycles of PCR using Takara *Taq* DNA polymerase (Takara, Japan) according to the supplier's instructions, with annealing at 60°C and elongation at 72°C for 30 s. PCR products were separated on a 1.5% agarose gel and visualized with ethidium bromide. For Southern blot analyses, digested DNA was separated on a 0.75% agarose gel, soaked in 0.25 M HCl for 15 min, and alkaline transferred onto nylon membranes (Boehringer Mannheim, Mannheim, Germany). The membranes were prehybridized in Hybrisol I

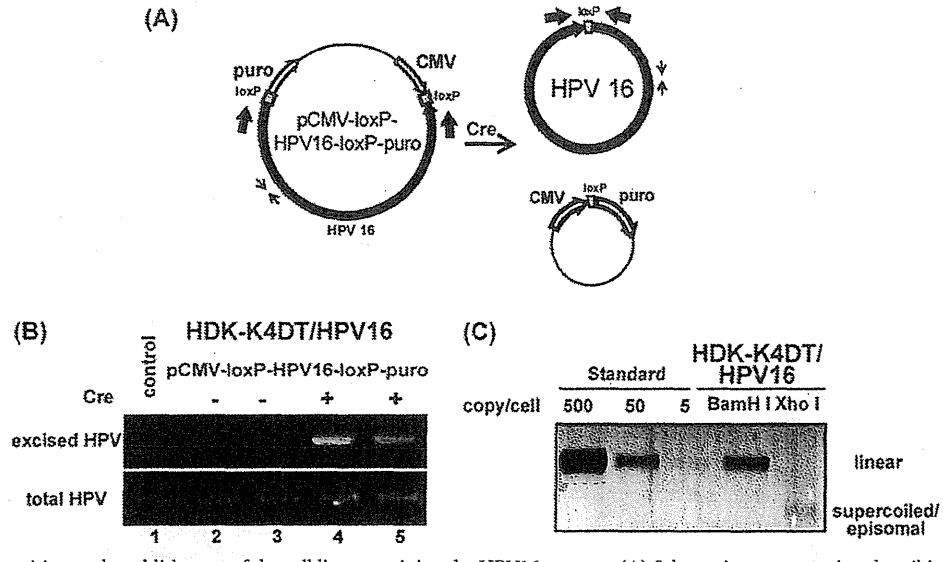

FIG 1 HPV genome excision and establishment of the cell line containing the HPV16 genome. (A) Schematic representation describing the parental pCMV-loxP-HPV16-loxP-puro, the Cre recombinase-excised HPV16 genome, and the pCMV-puro plasmid. PCR primers (thin and thick arrows) to detect total and excised HPV DNA, respectively, are indicated. (B) HDK-K4DT cells were cotransfected with the pCMV-loxP-HPV16-loxP-puro plasmid with (lanes 4 and 5) or without (lanes 2 and 3) the NCre expression plasmid. Total DNA was extracted from the cells 2 days after the transfection without puromycin selection. Representative pictures of an ethidium bromide-stained agarose gel with PCR products indicating total HPV16 DNA (bottom) and excised circular HPV16 DNA (top), containing a surplus of 34 bp of *loxP* DNA, are shown. (C) Southern blot hybridization for the HPV genome in HDK-K4DT cultures. DpnI and BamHI- or XhoI-digested total DNA isolated from HDK-K4DT at 3 weeks after transfection with pCMV-loxP-HPV16-loxP-puro plasmid and the NCre expression plasmid is shown. Digestion with BamHI, which cuts the HPV16 genome once, produced results of the expected size for the HPV16 genome. Digestion with XhoI, which does not cut the HPV16 genome, showed supercoiled plasmid of HPV16 genome. The BamHI-linearized HPV16 plasmid was used for length and copy number standards.

(Millipore, Billerica, MA) for 1 h at 42°C. A biotin-labeled probe of the entire HPV16 genome prepared with the NEBlot Phototope kit (New England BioLabs, Ipswich, MA) was applied for hybridization, and the hybridized DNA was visualized with a Phototope-Star detection kit (New England BioLabs) following the protocol provided by the manufacturer. The LAS3000 charge-coupled device (CCD) imaging system (Fujifilm Co. Ltd., Japan) was employed for detection and quantification.

RNA extraction and RT-PCR analyses. For detection of mRNAs, total RNA was purified with RNeasy (Qiagen, Valencia, CA) and reverse transcribed to generate cDNAs by the ThermoScript reverse transcription (RT)-PCR system (Invitrogen) using random hexamers according to the supplier's instructions. Primers used for the E1^E4 spliced transcript, exogenous codon optimized E1, and human acidic ribosomal phosphoprotein P0 (36B4) are shown in Table 1. The thermocycling profile for amplifying E1^E4, E1, and 36B4 cDNAs was 1 min at 95°C; 40 cycles of 95°C for 30 s, 54°C for 30 s, and 72°C for 30 s (or 1 min for E1^E4 cDNA); and 4 min of extension at 72°C. PCR products were separated in a 1.5 or 0.9% agarose gel and visualized with ethidium bromide.

Quantitative real-time PCR for genomic DNA. Reactions were prepared in a volume of 10 μl containing 1× quantitative PCR (qPCR) master mix of KAPA SYBR FAST qPCR kits (Kapa Biosystems, Woburn, MA) and 300 nM each primer. PCR was performed using StepOnePlus (Applied Biosystems) with 10 s of denaturation at 95°C followed by 40 cycles of 95°C for 3 s and 60°C for 30 s. Serial dilutions of linearized HPV16 genome from pUC-HPV16 plasmid DNA by BamHI digestion were used as controls to measure the amounts of HPV16 genomic DNA. All real-time PCRs were run in triplicate. Total DNA was digested with DpnI before PCR amplification of the HPV16 genome with a primer set amplifying a product containing two DpnI sites (Table 1). HPV16 DNA copy number was expressed as copies per cell assuming that the total human genomic DNA is 6.6 pg/diploid cell. The rate of HPV16 genome retention (RR) was calculated as follows: RR = (copy number of viral genomes at the end/copy number of viral genomes at the beginning) 1/PD, where population doubling (PD) of cells was calculated as follows: PD = log(number of cells obtained/initial number of cells)/log2.

RESULTS

Establishment of keratinocytes containing the HPV16 genome. Primary human keratinocytes are often used for establishment of HPV-containing cell lines. However, they have a finite life span, and cells harboring HPV genomes tend to preferentially grow in culture. To minimize this effect and to obtain reproducible results, we first immortalized human dermal keratinocytes (HDKs) with TERT, a mutant form of CDK4 and cyclin D1 (HDK-K4DT). HDK-K4DT formed fully stratified squamous epithelium in an organotypic raft culture (data not shown). Then, we established keratinocytes harboring HPV genomes as episomes. HDK-K4DT cells were transfected with pCMV-loxP-HPV16-loxP-puro, designed to generate a circular 7.9-Kb HPV16 genome and a circular pCMV-puro expression cassette (Fig. 1A). With the Cre expression plasmid, about 5 to 10% of the transfected cells survived after short-term puromycin selection, whereas only a few cells survived without Cre recombinase (data not shown). At 2 days posttransfection without puromycin selection, total DNA was analyzed by PCR using two sets of primers, one for total HPV16 DNA and the other specific for the circularized HPV16 genome (Fig. 1A). In cells cotransfected with Cre, PCR products corresponding to the recombined circular HPV16, whose size should be bigger by 34 bp due to an inserted *loxP* sequence, were observed (Fig. 1B, lanes 4 and 5), whereas no circularized HPV16 genome was detected in cells without Cre expression (Fig. 1B, lanes 2 and 3). Southern blot analysis of total DNA extracted from cells at 21 days posttransfection suggested that the established HDK-K4DT cells harbored

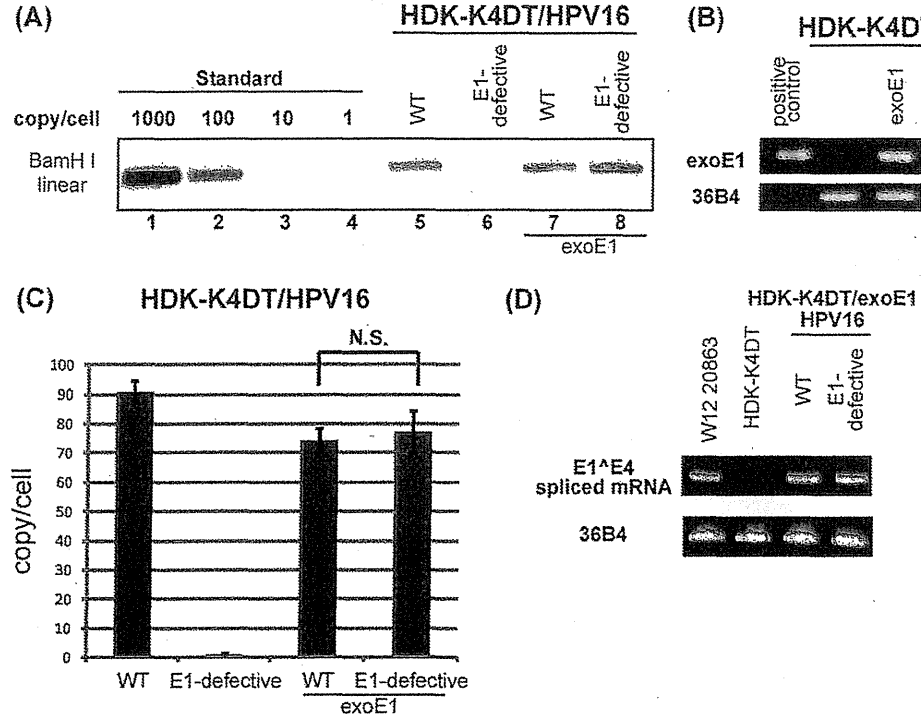

FIG 2 Requirement for E1 protein in the establishment stage. (A) Southern blot hybridization of the HPV genome in HDK-K4DT cultures. Parental (lanes 5 and 6) and exogenous E1 expressing HDK-K4DT cells (lanes 7 and 8) were transfected with the wild-type (WT) or the E1-defective pCMV-loxP-HPV16-loxP-puro plasmid and the NCre expression plasmid. Total DNA was extracted at 21 days posttransfection. DpnI- and BamHI-digested total DNA from parental or exogenous E1 expressing HDK-K4DT cultures was analyzed. The BamHI-linearized HPV16 plasmid was used for length and copy number standards (lanes 1 to 4). (B) mRNAs for exogenous E1 of HDK1-K4DT cells transduced with the retroviral vector expressing HA16E1 were analyzed. Total RNAs isolated from cells with or without the retroviral transduction were subjected to reverse transcription (RT)-PCR with a primer set specific to codon-optimized E1. 36B4 mRNA was also detected as an internal control. The PCR products of exogenous E1 (top) and 36B4 (bottom) visualized in ethidium bromide-stained agarose gels are shown. pCMSCV-FRT-HA16E1-TKneo-FRT was used as a positive control. (C) The copy number of the HPV16 genomes at 14 days posttransfection in each HDK-K4DT cell lines was determined by real-time PCR. The deviations of three independent sets of transfectants are shown as error bars. N.S., not significant. (D) Expression of the E1^E4 spliced mRNAs in E1-expressing HDK-K4DT cells harboring the wild type or the E1-defective HPV16 genomes at 35 days posttransfection. Total RNAs were subjected to RT-PCR with an E1^E4-specific primer set (Table 1). RNAs from parental HDK-K4DT cells and W12 cells were used as controls. PCR products of E1^E4 (top) and 36B4 (bottom) are shown, as described for panel B.

more than 50 viral genome copies per cell (Fig. 1C). Repeated transfection experiments confirmed the reproducibility of this technique. At 60 days posttransfection, after nine serial passages at a ratio of 1:8, we still detected 10 to 20 copies of the viral genomes per cell (data not shown). The rate of HPV16 genome retention was calculated as 90% per cell division.

E1 protein is required for establishment of HPV16 genomes as episomes in HDK-K4DT cells. To study the role of E1 in each stage of the viral life cycle, we prepared an E1-defective mutant HPV16 genome containing an E1 translation termination mutation at nt 892 to 894 to abrogate E1 protein expression. Unlike the wild-type HPV16 genome, the HPV16 E1-defective genome failed to establish in HDK-K4DT cells as episomes (Fig. 2A, lanes 5 and 6). However, in HDK-K4DT cells expressing exogenous E1 from the retrovirus, MSCV-FRT-HA16E1-TKneo-FRT, the E1-defective HPV16 genome could establish as episomes as efficiently as the wild type HPV16 genome (Fig. 2A, lanes 7 and 8). We confirmed the expression of exogenous E1 driven by the LTR promoter by RT-PCR using primers specific for exogenous E1 (Fig. 2B), though the E1 protein was undetectable by Western blot analysis. The copy numbers of the E1-defective HPV16 genome were comparable to that of the wild-type HPV16 genome in the presence of exogenous E1 expression (Fig. 2C). The translation termination mutation inserted in the downstream of the splice donor site for E1^E4 (nt 880) did not disrupt normal E1^E4 splicing (Fig. 2D). These data indicate that the E1 protein is required for initial replication and/or maintenance of the viral genome.

E1 protein is dispensable for maintenance replication of the viral genome. In order to assess the requirement of E1 protein for maintenance replication of the viral genome, we used the HDK-K4DT cells harboring the E1-defective HPV16 genomes established with exogenous E1 expression from the integrated MSCV-FRT-HA16E1-TKneo-FRT retrovirus. Upon infection of FLPe-expressing AdV, the exogenous E1 expression cassette as well as the TKneo gene was excised by FLP at an efficiency of around 50% (Fig. 3A). Then we isolated HDK-K4DT cells which no longer expressed exogenous E1 by ganciclovir selection (Fig. 3B). After several passages of cells at a ratio of 1:8, the copy number of HPV16 genomes was determined by real-time PCR. We detected 70 to 100 copies of the wild-type or the E1-defective HPV16 genomes per cell just before the AdV infection. Copy numbers of both the wild-type and the E1-defective HPV16 genomes gradually decreased during the passages (Fig. 3C). However, about 10 to 20 copies of the E1-defective HPV16 genomes

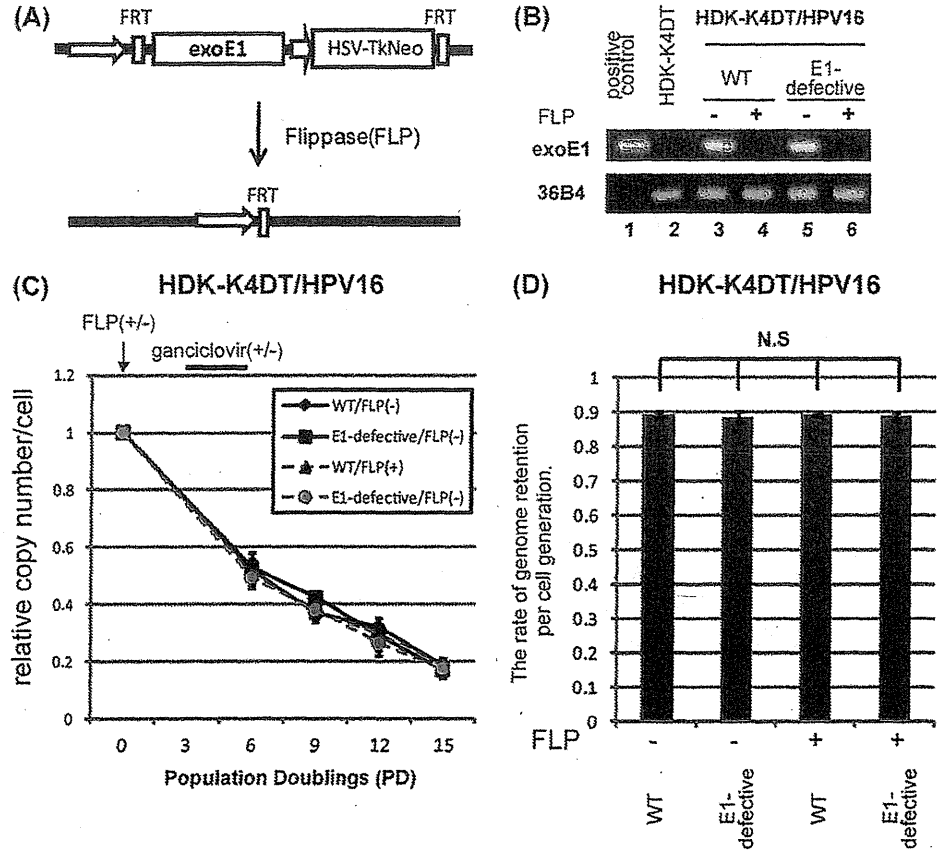

FIG 3 E1 protein is not essential for maintenance replication of the viral genome. (A) Schematic representation of the viral vector, MSCV-FRT-HA16E1-TKneo-FRT, expressing exogenous E1. The HA-tagged HPV16 E1 gene and the TKneo fusion gene are flanked by FLP recognition target (FRT) sites. When a thermostable FLP-expressing AdV (AxCAFLPe) is infected, the DNA in between the FRT sites is excised so that exogenous E1 as well as TKneo expression is terminated. Cells still expressing E1 and HSV-TK can be negatively selected with ganciclovir. (B) mRNAs containing exogenous E1 message were analyzed to ensure complete removal of E1 expression. Total RNAs isolated from HDK-K4DT/HPV16 cell lines at 21 days postinfection with (lanes 4 and 6) or without (lanes 3 and 5) AxCAFLPe were subjected to RT-PCR with a primer set specific to codon-optimized E1. Representative pictures of an ethidium bromide-stained agarose gel with PCR products indicating exogenous E1 (top) and 36B4 (an internal control; bottom) are shown. pCMSCV-FRT-HA16E1-TKneo-FRT was used as a positive control. (C) HDK-K4DT cells containing the wild type (WT) or the E1-defective HPV16 genome were established in the presence of exogenous E1 expression. Two weeks after transfection, aliquots of cells were infected with AxCAFLPe (FLP +) at a multiplicity of infection of 5, followed by selection with 10 μg/ml of ganciclovir for 1 week. After the selection, cells were cultured for 4 passages at a ratio of 1:8 to examine the retention rate of the wild-type or the E1-defective genome in the presence or the absence of exogenous E1. HDK-K4DT/HPV16 cells which were not infected with AxCAFLPe (FLP−) were also cultured for 5 passages at a ratio of 1:8. Total DNA was extracted just before the infection, at every passage and at the end of the culture. The copy number of HPV16 genomes was measured by real-time PCR and normalized to the total amount of DNA. The graph shows time courses of copy number change during the 5 passages after the infection. The copy number at the each time point is shown as a ratio to the copy number just before the FLP-expressing adenovirus infection (PD0). The end of the ganciclovir selection corresponds to PD6. Means and standard errors of the means are shown. (D) The graph shows the rates of HPV genome retention per cell division. The retention rates were calculated as described in Materials and Methods. Means from three independent experiments and standard deviations are shown as error bars. N.S., not significant, compared with each other.

per cell still remained after several passages of cells, even in the absence of exogenous E1 expression. No difference in the rate of genome retention was observed between the E1-defective and the wild-type HPV16 genomes. The rates were calculated as approximately 90% per cell division, irrespective of exogenous E1 expression, and proved quite constant in three independent experiments (Fig. 3D). These data indicate that the E1 protein is dispensable for maintenance replication of the viral genome.

E1 protein is required for viral genome amplification upon differentiation. To confirm that E1 protein is required for the productive stage of viral replication, differentiation-dependent viral genome amplification was examined with the same series of the cells established for the previous section (Fig. 3). HDK-K4DT cells harboring the wild-type or the E1-defective HPV16 genomes in the presence or the absence of exogenous E1 expression were exposed to a high calcium concentration. Induction of differentiation was confirmed by expression of keratinocyte differentiation markers, involucrin and loricrin (Fig. 4A). Southern blot analyses of DNA extracted from sister cultures showed the wild-type HPV16 genomes to be amplified episomally upon differentiation in the absence of exogenous E1 expression (Fig. 4B, lanes 1 to 2). However, the E1-defective HPV16 genomes were amplified only in the presence of exogenous E1 expression (Fig. 4B, lanes 3 to 6). Reintroduction of E1 with lentiviruses, CSII-CMV-tetON and CSII-TRE-Tight-HA16E1, to the cells whose exogenous E1 cassette had been excised by FLP rescued the E1-defective HPV16 genome amplification upon differentiation only when the E1 expression was induced by doxycycline (Fig. 4B, lanes 7 and 8),

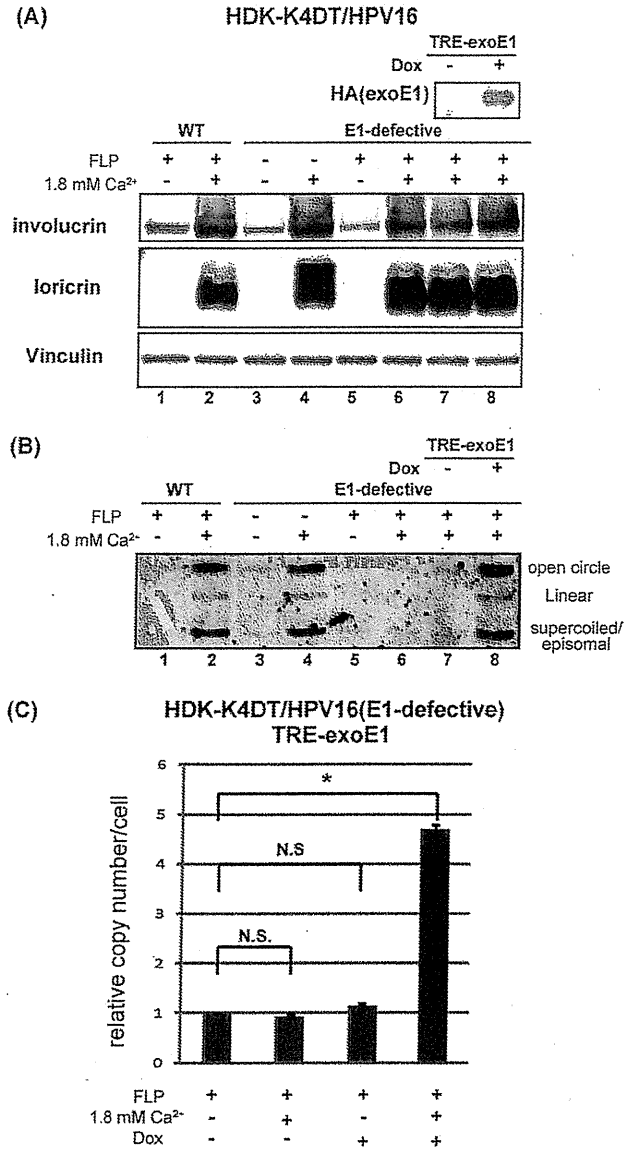

FIG 4 E1 protein is required for viral genome amplification upon differentiation. (A) HDK-K4DT cells harboring the wild-type (lanes 1 and 2) or the E1-defective (lanes 3 to 8) HPV16 genomes in the presence (FLP−, lanes 3 and 4) or the absence (FLP+, lanes 1 and 2, 5 to 8) of exogenous E1 expression were seeded at 2×10^5 cells per well (6-well plate) in Epilife complete growth medium, and then cells were exposed to 1.8 mM calcium (lanes 2, 4, 6, 7, 8) to induce keratinocyte differentiation. Total cell lysates were made, and total DNAs were extracted from the sister cultures just before and 10 days after calcium exposure. The expression of involucrin and loricrin, keratinocyte differentiation markers, was analyzed by Western blotting. Expression of reintroduced exogenous E1 controlled by doxycycline was detected by anti-HA antibody (lanes 7 and 8). Vinculin was detected as a loading control. (B) Southern blot hybridization for episomal HPV16 genomes in HDK-K4DT cells. XhoI-digested total DNA from each HDK-K4DT culture was loaded. A representative image of three independent experiments is shown. (C) The copy number of the E1-defective HPV16 genomes in HDK-K4DT cells in the indicated condition was determined by real-time PCR. Three replicates are shown and standard deviations are shown as error bars. N.S., not significant. The single asterisk indicates P values of <0.05.

whereas induction of E1 alone without high calcium failed to rescue the genome amplification (Fig. 4C). These data indicate that E1 protein is required for viral genome amplification upon differentiation. Since the same series of cells used for Fig. 3 were used in these experiments, the results confirmed that the E1-defective HPV16 genomes were episomally maintained in the absence of E1 expression.

DISCUSSION

In this study, we demonstrated that E1 is dispensable for maintenance replication of the HPV16 genome but required for replication in the establishment and productive stages. Taking the previous study using a TS E1 mutant of BPV1 (17) into account, it is likely that E1 is dispensable for the maintenance replication of other PVs, too.

Thus, HPVs have at least two replication modes and control the copy number of the viral genome depending on the situation. Such a strategy of the virus would clearly be beneficial for persistent infection and continuous virus production. In the maintenance phase, minimal expression of viral proteins in host cells with low copy numbers of viral genomes would allow HPV to evade cellular immune surveillance. Moreover, as recent studies indicate, a high level of E1 expression in basal-layer cells could activate an ATM-dependent damage response and cause growth suppression (10, 32).

It is reasonable to speculate that the E1-independent maintenance replication employs the cellular replication machinery to support viral genome maintenance under S phase control. Mechanisms of viral genome DNA replication control by host cell factors have been well studied for the Epstein-Barr virus (EBV). The EBV genome DNA is replicated once per S phase in the latent phase of infection (19, 44). In this phase, EBV employs replication licensing proteins, MCMs and ORC (19, 22), which assemble on the latent origin of replication of EBV, OriP. A low copy number for the viral genome may be an appropriate common strategy for episomal viruses to sustain latent infection. Although it is not known whether and how MCMs and ORC are involved in HPV DNA replication, E1- and E2-independent *cis*-replicating elements may reside outside the LCR and possibly in the late region (L2-L1 open reading frames [ORFs]) of the HPV16 genome (28, 29).

The observed rate of HPV16 genome retention was about 90% per cell generation, which is comparable to the reported rate for the EBV genome (25). With this retention rate, the viral genomes of 100 copies per cell can be maintained for 2 to 3 months, corresponding to approximately 40 cell divisions under our culture conditions. In the stratified squamous epithelium, stem cells self-renew by dividing infrequently and generate a population of cells that undergo limited but more frequent divisions before giving rise to nonproliferative, terminally differentiating cells. In the natural life cycle of HPVs, the virus must infect epithelial stem cells (8, 34), which would divide much less frequently than cultured cells do. Therefore, the viral genome in the stem cells *in vivo* would be able to persist for much longer period than in cultured cells, even if the genome retention rate is the same as that found in our study.

In maintenance replication, HPV may still employ two different modes of replication. Hoffmann et al. showed that HPV16 DNA replicates once per S phase in W12 cells, while HPV31 DNA replicates via a random-choice mechanism with some multiple

rounds of the viral genome replication per S phase in CIN612-9E cells, and that forced expression of E1 in W12 cells converted HPV16 DNA replication to random-choice replication (12). Interestingly, when HPV16 or HPV31 DNAs are separately introduced into NIKS cells, they both replicate randomly (12). Thus, it is likely that the difference between W12 and CIN612-9E cells depends on expression levels of E1. It is possible that occasional or low-level expression of auxiliary E1 hinders the copy number loss for an even longer period of maintenance, as indicated by previous studies (18, 39). Theoretically, E1 protein could be supplied from the infected virion and/or by *de novo* synthesis from the infected viral genome in the establishment stage. In this regard, it is not clear whether our experimental system recapitulates the actual establishment stage of the HPV life cycle, since E1 can be supplied only by *de novo* synthesis. At present, little is known about the underlying mechanisms of the establishment stage and the mechanism(s) of switching to the subsequent maintenance stage. Clearly, it needs to be examined whether the E1 protein is included in infectious virions and how the E1 expression is regulated in the three different stages.

PV E1 protein forms double hexamers at the replication origin in the LCR with the help of E2 (2, 11, 43) and unwinds DNA through helicase activity ahead of replication forks powered by the hydrolysis of ATP (31). Since E1 is the only viral protein with enzymatic activities, it is an attractive target for development of novel therapeutic agents to treat HPV-associated benign lesions where the whole viral life cycle is completed. Indeed, some candidate small molecules have been reported to inhibit the E1 function (5, 9, 15, 40–42). However, their identification and evaluation was done using biochemical assays or surrogate cell-based assays, and a true antiviral activity has yet to be tested. Based on our present study, the effectiveness of E1 inhibitors as antiviral drugs may be restricted, since they cannot inhibit E1-independent HPV replication in long-living basal cells. Inhibition of E1 protein function could prevent amplification of the viral genome in the establishment and productive stages. Thus, it may prevent HPV infection and reduce pathogenesis, including papilloma formation and virion production. In the case of cervical intraepithelial neoplasias (CINs), continuous inhibition of E1 might reverse low-grade lesions to apparently healthy mucosa, but interruption of the inhibition might lead to recurrence of the lesions. More importantly, it may not be able to eliminate the HPV genomes replicating in undifferentiated basal cells, which are thought to be the histogenetic origin of cervical cancer. Thus, E1 inhibition might not be able to prevent CIN lesions from progressing into cancer.

In summary, we have established an experimental system which can evaluate the requirement of any viral gene of interest in the viral life cycle by supplying and deleting exogenous expression of the gene and demonstrated that E1 is entirely dispensable for maintenance replication of the HPV16 genome in human keratinocytes. Thus, inhibition of E1 may not be able to eliminate the viral genome from the basal cell layer. The rationale for development of E1 inhibitors as anti-HPV drugs may be more restricted than formerly envisaged. Further studies will be required to elucidate the roles of cellular replication factors and the *cis* elements of the HPV genome in E1-independent maintenance replication.

ACKNOWLEDGMENTS

We express our appreciation to Takako Ishiyama for expert technical assistance. We are grateful to John H. Lee (University of Iowa Hospitals and Clinics) for the loxP-HPV16-loxP construct, Izumu Saito (University of Tokyo and RIKEN RDB) for adenovirus vectors, and Hiroyuki Miyoshi (RIKEN BRC) for lentivirus vectors and packaging constructs.

This work was supported in part by Grants-in-Aid for Cancer Research from the Ministry of Health Labor and Welfare to T.K., and for Scientific Research from the Ministry of Education, Culture, Sports, Science, and Technology of Japan to N.E., T.N., and T.K.

REFERENCES

1. Angeletti PC, Kim K, Fernandes FJ, Lambert PF. 2002. Stable replication of papillomavirus genomes in *Saccharomyces cerevisiae*. J. Virol. 76:3350–3358.
2. Berg M, Stenlund A. 1997. Functional interactions between papillomavirus E1 and E2 proteins. J. Virol. 71:3853–3863.
3. Buchholz F, Angrand PO, Stewart AF. 1998. Improved properties of FLP recombinase evolved by cycling mutagenesis. Nat. Biotechnol. 16:657–662.
4. Chiang CM, et al. 1992. Viral E1 and E2 proteins support replication of homologous and heterologous papillomaviral origins. Proc. Natl. Acad. Sci. U. S. A. 89:5799–5803.
5. D'Abramo CM, Archambault J. 2011. Small molecule inhibitors of human papillomavirus protein-protein interactions. Open Virol. J. 5:80–95.
6. Del Vecchio AM, Romanczuk H, Howley PM, Baker CC. 1992. Transient replication of human papillomavirus DNAs. J. Virol. 66:5949–5958.
7. Doorbar J. 2006. Molecular biology of human papillomavirus infection and cervical cancer. Clin. Sci. (Lond.) 110:525–541.
8. Egawa K. 2003. Do human papillomaviruses target epidermal stem cells? Dermatology 207:251–254.
9. Faucher AM, et al. 2004. Discovery of small-molecule inhibitors of the ATPase activity of human papillomavirus E1 helicase. J. Med. Chem. 47:18–21.
10. Fradet-Turcotte A, et al. 2011. Nuclear accumulation of the papillomavirus E1 helicase blocks S-phase progression and triggers an ATM-dependent DNA damage response. J. Virol. 85:8996–9012.
11. Frattini MG, Laimins LA. 1994. Binding of the human papillomavirus E1 origin-recognition protein is regulated through complex formation with the E2 enhancer-binding protein. Proc. Natl. Acad. Sci. U. S. A. 91:12398–12402.
12. Hoffmann R, Hirt B, Bechtold V, Beard P, Raj K. 2006. Different modes of human papillomavirus DNA replication during maintenance. J. Virol. 80:4431–4439.
13. Jeon S, Lambert PF. 1995. Integration of human papillomavirus type 16 DNA into the human genome leads to increased stability of E6 and E7 mRNAs: implications for cervical carcinogenesis. Proc. Natl. Acad. Sci. U. S. A. 92:1654–1658.
14. Kanegae Y, et al. 1996. Efficient gene activation system on mammalian cell chromosomes using recombinant adenovirus producing Cre recombinase. Gene 181:207–212.
15. Kasukawa H, Howley PM, Benson JD. 1998. A fifteen-amino-acid peptide inhibits human papillomavirus E1–E2 interaction and human papillomavirus DNA replication in vitro. J. Virol. 72:8166–8173.
16. Kim K, Angeletti PC, Hassebroek EC, Lambert PF. 2005. Identification of *cis*-acting elements that mediate the replication and maintenance of human papillomavirus type 16 genomes in *Saccharomyces cerevisiae*. J. Virol. 79:5933–5942.
17. Kim K, Lambert PF. 2002. E1 protein of bovine papillomavirus 1 is not required for the maintenance of viral plasmid DNA replication. Virology 293:10–14.
18. Lee JH, et al. 2004. Propagation of infectious human papillomavirus type 16 by using an adenovirus and Cre/LoxP mechanism. Proc. Natl. Acad. Sci. U. S. A. 101:2094–2099.
19. Lindner SE, Sugden B. 2007. The plasmid replicon of Epstein-Barr virus: mechanistic insights into efficient, licensed, extrachromosomal replication in human cells. Plasmid 58:1–12.
20. Lu JZ, Sun YN, Rose RC, Bonnez W, McCance DJ. 1993. Two E2 binding sites (E2BS) alone or one E2BS plus an A/T-rich region are minimal requirements for the replication of the human papillomavirus type 11 origin. J. Virol. 67:7131–7139.
21. Maglennon GA, McIntosh P, Doorbar J. 2011. Persistence of viral DNA in the epithelial basal layer suggests a model for papillomavirus latency following immune regression. Virology 414:153–163.

22. Maiorano D, Lemaitre JM, Mechali M. 2000. Stepwise regulated chromatin assembly of MCM2-7 proteins. J. Biol. Chem. 275:8426–8431.
23. Mungal S, Steinberg BM, Taichman LB. 1992. Replication of plasmid-derived human papillomavirus type 11 DNA in cultured keratinocytes. J. Virol. 66:3220–3224.
24. Nakano M, Ishimura M, Chiba J, Kanegae Y, Saito I. 2001. DNA substrates influence the recombination efficiency mediated by FLP recombinase expressed in mammalian cells. Microbiol. Immunol. 45:657–665.
25. Nanbo A, Sugden A, Sugden B. 2007. The coupling of synthesis and partitioning of EBV's plasmid replicon is revealed in live cells. EMBO J. 26:4252–4262.
26. Narisawa-Saito M, et al. 2007. HPV16 E6-mediated stabilization of ErbB2 in neoplastic transformation of human cervical keratinocytes. Oncogene 26:2988–2996.
27. Naviaux RK, Costanzi E, Haas M, Verma IM. 1996. The pCL vector system: rapid production of helper-free, high-titer, recombinant retroviruses. J. Virol. 70:5701–5705.
28. Pittayakhajonwut D, Angeletti PC. 2008. Analysis of *cis*-elements that facilitate extrachromosomal persistence of human papillomavirus genomes. Virology 374:304–314.
29. Pittayakhajonwut D, Angeletti PC. 2010. Viral *trans*-factor independent replication of human papillomavirus genomes. Virol. J. 7:123.
30. Rabson MS, Yee C, Yang YC, Howley PM. 1986. Bovine papillomavirus type 1 3′ early region transformation and plasmid maintenance functions. J. Virol. 60:626–634.
31. Rocque WJ, et al. 2000. Replication-associated activities of purified human papillomavirus type 11 E1 helicase. Protein Expr. Purif. 18:148–159.
32. Sakakibara N, Mitra R, McBride A. 2011. The papillomavirus E1 helicase activates a cellular DNA damage response in viral replication foci. J. Virol. 85:8981–8995.
33. Sasaki R, et al. 2009. Oncogenic transformation of human ovarian surface epithelial cells with defined cellular oncogenes. Carcinogenesis 30:423–431.
34. Schmitt A, et al. 1996. The primary target cells of the high-risk cottontail rabbit papillomavirus colocalize with hair follicle stem cells. J. Virol. 70: 1912–1922.
35. Sverdrup F, Khan SA. 1994. Replication of human papillomavirus (HPV) DNAs supported by the HPV type 18 E1 and E2 proteins. J. Virol. 68:505–509.
36. Takata Y, Kondo S, Goda N, Kanegae Y, Saito I. 2011. Comparison of efficiency between FLPe and Cre for recombinase-mediated cassette exchange in vitro and in adenovirus vector production. Genes Cells 16:765–777.
37. Ustav M, Stenlund A. 1991. Transient replication of BPV-1 requires two viral polypeptides encoded by the E1 and E2 open reading frames. EMBO J. 10:449–457.
38. Ustav M, Ustav E, Szymanski P, Stenlund A. 1991. Identification of the origin of replication of bovine papillomavirus and characterization of the viral origin recognition factor E1. EMBO J. 10:4321–4329.
39. Wang HK, Duffy AA, Broker TR, Chow LT. 2009. Robust production and passaging of infectious HPV in squamous epithelium of primary human keratinocytes. Genes Dev. 23:181–194.
40. White PW, Faucher AM, Goudreau N. 2011. Small molecule inhibitors of the human papillomavirus E1-E2 interaction. Curr. Top. Microbiol. Immunol. 348:61–88.
41. White PW, et al. 2005. Biphenylsulfonacetic acid inhibitors of the human papillomavirus type 6 E1 helicase inhibit ATP hydrolysis by an allosteric mechanism involving tyrosine 486. Antimicrob. Agents Chemother. 49: 4834–4842.
42. White PW, et al. 2003. Inhibition of human papillomavirus DNA replication by small molecule antagonists of the E1-E2 protein interaction. J. Biol. Chem. 278:26765–26772.
43. Yang L, Li R, Mohr IJ, Clark R, Botchan MR. 1991. Activation of BPV-1 replication in vitro by the transcription factor E2. Nature 353:628–632.
44. Yates JL, Guan N. 1991. Epstein-Barr virus-derived plasmids replicate only once per cell cycle and are not amplified after entry into cells. J. Virol. 65:483–488.
45. zur Hausen H. 2002. Papillomaviruses and cancer: from basic studies to clinical application. Nat. Rev. Cancer 2:342–350.

OPEN ACCESS Freely available online

PLoS one

Establishment of Functioning Human Corneal Endothelial Cell Line with High Growth Potential

Tadashi Yokoi[1,2], Yuko Seko[1,7], Tae Yokoi[1], Hatsune Makino[3], Shin Hatou[4], Masakazu Yamada[5], Tohru Kiyono[6], Akihiro Umezawa[3], Hiroshi Nishina[2], Noriyuki Azuma[1]*

1 Department of Ophthalomology, National Center for Child Health and Development, Tokyo, Japan, **2** Department of Developmental and Regenerative Biology, Medical Research Institute, Tokyo Medical and Dental University, Bunkyo-ku Tokyo, Japan, **3** Department of Reproductive Biology, National Research Institute for Child Health and Development, Tokyo, Japan, **4** Department of Ophthalmology, Keio University School of Medicine, Tokyo, Japan, **5** Division for Vision Research, National Institute of Sensory Organs, National Tokyo Medical Center, Tokyo, Japan, **6** Division of Virology, National Cancer Center Research Institute, Tokyo, Japan, **7** Sensory Functions Section, Research Institute, National Rehabilitation Center for Persons with Disabilities, Tokyo, Japan

Abstract

Hexagonal-shaped human corneal endothelial cells (HCEC) form a monolayer by adhering tightly through their intercellular adhesion molecules. Located at the posterior corneal surface, they maintain corneal translucency by dehydrating the corneal stroma, mainly through the Na^+- and K^+-dependent ATPase (Na^+/K^+-ATPase). Because HCEC proliferative activity is low *in vivo*, once HCEC are damaged and their numbers decrease, the cornea begins to show opacity due to overhydration, resulting in loss of vision. HCEC cell cycle arrest occurs at the G1 phase and is partly regulated by cyclin-dependent kinase inhibitors (CKIs) in the Rb pathway (p16-CDK4/CyclinD1-pRb). In this study, we tried to activate proliferation of HCEC by inhibiting CKIs. Retroviral transduction was used to generate two new HCEC lines: transduced human corneal endothelial cell by human papillomavirus type E6/E7 (THCEC (E6/E7)) and transduced human corneal endothelial cell by Cdk4R24C/CyclinD1 (THCEH (Cyclin)). Reverse transcriptase polymerase chain reaction analysis of gene expression revealed little difference between THCEC (E6/E7), THCEH (Cyclin) and non-transduced HCEC, but cell cycle-related genes were up-regulated in THCEC (E6/E7) and THCEH (Cyclin). THCEH (Cyclin) expressed intercellular molecules including ZO-1 and N-cadherin and showed similar Na^+/K^+-ATPase pump function to HCEC, which was not demonstrated in THCEC (E6/E7). This study shows that HCEC cell cycle activation can be achieved by inhibiting CKIs even while maintaining critical pump function and morphology.

Citation: Yokoi T, Seko Y, Yokoi T, Makino H, Hatou S, et al. (2012) Establishment of Functioning Human Corneal Endothelial Cell Line with High Growth Potential. PLoS ONE 7(1): e29677. doi:10.1371/journal.pone.0029677

Editor: Irina Kerkis, Instituto Butantan, Brazil

Received July 18, 2011; **Accepted** December 2, 2011; **Published** January 19, 2012

Funding: This study was supported by a grant (#18390473) from the Ministry of Education, Culture, Sports, Science and Technology (MEXT) of Japan. The funders had no role in study design, data collection and analysis, decision to publish, or preparation of the manuscript.

Competing Interests: The authors have declared that no competing interests exist.

* E-mail: azuma-n@ncchd.go.jp

Introduction

Human corneal endothelial cells (HCEC) are hexagonal in shape and form a fragile monolayer lying posterior to the surface of the cornea. These cells maintain corneal transparency by their tight intercellular barrier and perform an ion transport pump function through Na^+/K^+-ATPase, which regulates the hydration of the corneal stroma [1,2]. If HCEC sustain damage, excessive hydration and opacity of the cornea occur, resulting in decreased vision.

Corneal endothelia are believed not to increase in adult humans and in fact gradually decrease by approximately 0.5% per year [3,4,5]. Damage, injury or HCEC disease such as Fuchs' corneal dystrophy [6], diabetes [7], trauma [8], cataract surgery [9] or elevation of intraocular pressure [10] does not lead to increased proliferation but rather to an increase in cell size to compensate for the wounded area [11]. Once the cell number falls below 1,000 cells/mm^2, the monolayer of enlarged HCEC cannot maintain corneal translucency [12] and surgical treatment is required to restore vision.

Penetrating keratoplasty has long been the surgical treatment of choice, involving replacement of a total layer of cornea by donor material. However, it can also result in adverse effects such as astigmatism and severe rejection requiring long term usage of immunosuppressive drugs [13]. Recently, alternative transplantation strategies, including modified posterior lamellar keratoplasty techniques such as deep lamellar endothelial keratoplasty (DLEK) [14], Descemet's stripping with endothelial keratoplasty (DSEK) [15] and Descemet membrane endothelial keratoplasty (DMEK) [16] have been introduced to overcome these problems. Despite these advances, an increasingly aging population requiring corneal transplants and inadequate tissue quality limit the availability of donor corneas, such that alternative ways of preparing endothelial cell monolayers need to be explored.

HCEC were originally believed to be incapable of expanding *in vitro*, but have been successfully isolated and cultured by introducing stimulating agents such as epidermal growth factor, platelet-derived growth factor-BB, bovine pituitary extract and fetal bovine serum [17,18]. However, the number of cells with proliferative activity and the ability to respond to such agents is relatively low, and much variation in proliferative activity exists between donors of different ages [19,20]. Thus, there is a requirement to achieve a stable and effective culture of cells in terms of both cell proliferation and physiologic function.

The HCEC cell cycle is mainly regulated by the p53 and pRB pathways, both of which have been inactivated by human papilloma virus (HPV) type 16 E6/E7 to successfully immortalize cells. Kim et al. reported the establishment of an immortalized HCEC line using HPV type 16 E6/E7 on lyophilized human amniotic membrane [21]. However, several studies have reported carcinogenesis of the cell line established by viral oncogenes including HPV type 16 E6/E7 or SV40 large T antigen [22,23]. Therefore a corneal endothelial cell line developed in this way does not appear to be suitable for the treatment of human corneal diseases. To resolve this problem, we expressed mutant cyclin-dependent kinase (Cdk) 4 and CyclinD1 to inactivate the pRB pathway and generate corneal endothelial cell lines without transducing viral oncogenes.

Results

HCEC with Descemet's membranes were proliferated slowly in a culture dish coated in type IV collagen. After two passages, the cells were transferred into 24-well dishes and transfected with a retroviral vector carrying E6/E7 or mutant Cdk4 and CyclinD1. Three cell lines were successfully generated, as shown in Fig. 1A, with obvious differences in growth (Fig. 1B). Protein expression from the transduced gene was confirmed by western blotting (Fig. 1C). As previously reported [21], THCEC (E6/E7) was immortalized, and THCEC (Cyclin) demonstrated the same proliferative capacity as THCEC (E6/E7), while primary cells grew more slowly even when cultured in 10% fetal bovine serum. These results indicate that induction of mutant Cdk4 and CyclinD1 is sufficient to generate a HCEC line that proliferates at a faster rate than the primary cell line.

Proliferation capacity was also confirmed by immunohistochemistry of Ki-67 (Fig. 2A). Expression of downstream genes of CyclinD1 which are associated with cell proliferation was analyzed by real-time polymerase chain reaction (PCR) (Fig. 2B). Positive staining of Ki-67, which is detected in the nucleus, was confirmed in both THCEC (Cyclin) and THCEC (E6/E7). Real-time PCR also revealed that CDC2 and PCNA, target genes of E2F (an upstream transcriptional factor), that are activated by CyclinD1, were up-regulated in THCEC (E6/E7) and especially in THCEC (Cyclin).

Expression of genes involved in active transmembrane transporter activity, including Na^+/K^+-ATPase, or cell adhesion, including ZO-1 and N-cadherin, were assessed by semi-quantitative reverse transcriptase (RT)-PCR (Fig. 3A). Expression of intercellular adhesion molecules was confirmed by immunohistochemistry (Fig. 3B–J). Semi-quantitative RT-PCR showed that there was no significant difference between the three cell lines regarding the expression of genes associated with several molecules of cell adhesion or of ion transporter channels, which are characteristically expressed by HCEC [21,24]. This was also confirmed by real-time PCR (data not shown).

ZO-1 and N-cadherin, key HCEC adhesion molecules [24], demonstrated positive staining at the intercellular junction in HCEH (Fig. 3F, I) and THCEC (Cyclin) (Fig. 3E, H), while neither ZO-1 nor N-cadherin was detected in THCEC (E6/E7) despite sufficient cellular density (Fig. 3G, J). Although positive staining of ZO-1 and N-cadherin was observed at the intercellular junction in THCEC (Cyclin), ZO-1 staining also occurred around the nucleus (Fig. 3E), indicating the immature distribution of the ZO-1 protein. In THCEC (Cyclin) and HCEC, hexagonal morphology was identified both by phase-contrast micrography (Fig. 3B, C) and immunocytochemistry, while the structure of hexagonal cell shape was not maintained in THCEC (E6/E7) (Fig. 3D). These data indicate that THCEC (Cyclin) and HCEC, but not THCEC (E6/E7), maintain contact inhibition which is crucial for preserving the monolayer.

Scanning electron microscopy was performed to reveal detailed information on the cellular junction (Fig. 4). THCEC (Cyclin) and HCEC showed a clear cellular junction including a tight junction, whereas THCEC (E6/E7) grew as a multilayer without forming a cellular junction, which confirms the immunohistochemistry result.

Representative traces of circuit current driven by the Na^+/K^+-ATPase were of similar shapes in both HCEC and THCEC (Cyclin) (Fig. 5A). These circuit currents maintain corneal translucency and their levels in both cell lines were clearly reduced by the presence of the Na^+/K^+-ATPase inhibitor ouabain, which confirms that the origin of the current is Na^+/K^+-ATPase. Meanwhile, the pump function in THCEC (Cyclin), detected in both earlier and later passages of cells, was more variable than that in HCEC (Fig. 5B), possibly indicating incomplete Na^+/K^+-ATPase activity or the presence of an intercellular barrier that regulates ion permeability. No regular circuit current was detected in THCEC (E6/E7) (Fig. 5A, B), which probably reflects the absence of intercellular adhesion preventing free ion transport across the membrane. This experiment clearly showed that the THCEC (Cyclin) monolayer has similar Na^+/K^+-ATPase activity to that of HCEC.

A tumorigenesis assay of nude mice detected no solid tumor in either THCEC (Cyclin) or THCEC (E6/E7), while HeLa cells formed a solid tumor in all mice (Table 1). Since THCEC (Cyclin) has a similar morphology and pump function to HCEC, THCEC (Cyclin) could be suitable for HCEC studies.

Discussion

THCEC (E6/E7) was shown to achieve immortalization with a highly activated proliferative capacity, as previously described [21]. However, the cell lines did not show normal intercellular contact or normal pump function, probably because contact inhibition in the cell line was not achieved. Meanwhile, THCEC (Cyclin) was demonstrated to have normal physiologic function with a greater proliferative capacity than primary cells, but slightly lower than that of THCEC (E6/E7).

In expanding the cellular life span, E7 has been shown to play a role in the inactivation of pRB, while E6 activates telomerase [25] and accelerates p53 degradation, which induces the Cdk inhibitor p21 [26]. However, little is known about the effector sites of the viral oncogene that may be related to genetic instability of immortalized cells. In the present study, expression of genes specific to HCEC was not drastically different between the three cell lines. However, key proteins including ZO-1 and N-cadherin that are important in forming intercellular contacts were detected, probably because of the unknown influence of viral oncogenes on post-translational modification, posttranslational import or protein stability/degradation.

We recently established genetically stable, non-transformed immortalized ovarian surface epithelium (OSE) cell lines without viral oncogenes by expressing mutant Cdk 4, CyclinD1 and hTERT, based on the hypothesis that inactivation of the pRb pathway and activation of telomerase are sufficient for OSE immortalization [27]. Meanwhile, Rane et al. demonstrated that mutant Cdk 4 (Cdk4R24C) is sufficient to induce carcinogenesis in several other tissues including those of the pancreas, pituitary and brain [28], and Joyce and colleagues showed that HCEC are arrested in the G1 phase and regulated by CKIs, p16INK4a and p21WAF1/Cip1 [29]. Considering the importance of maintaining

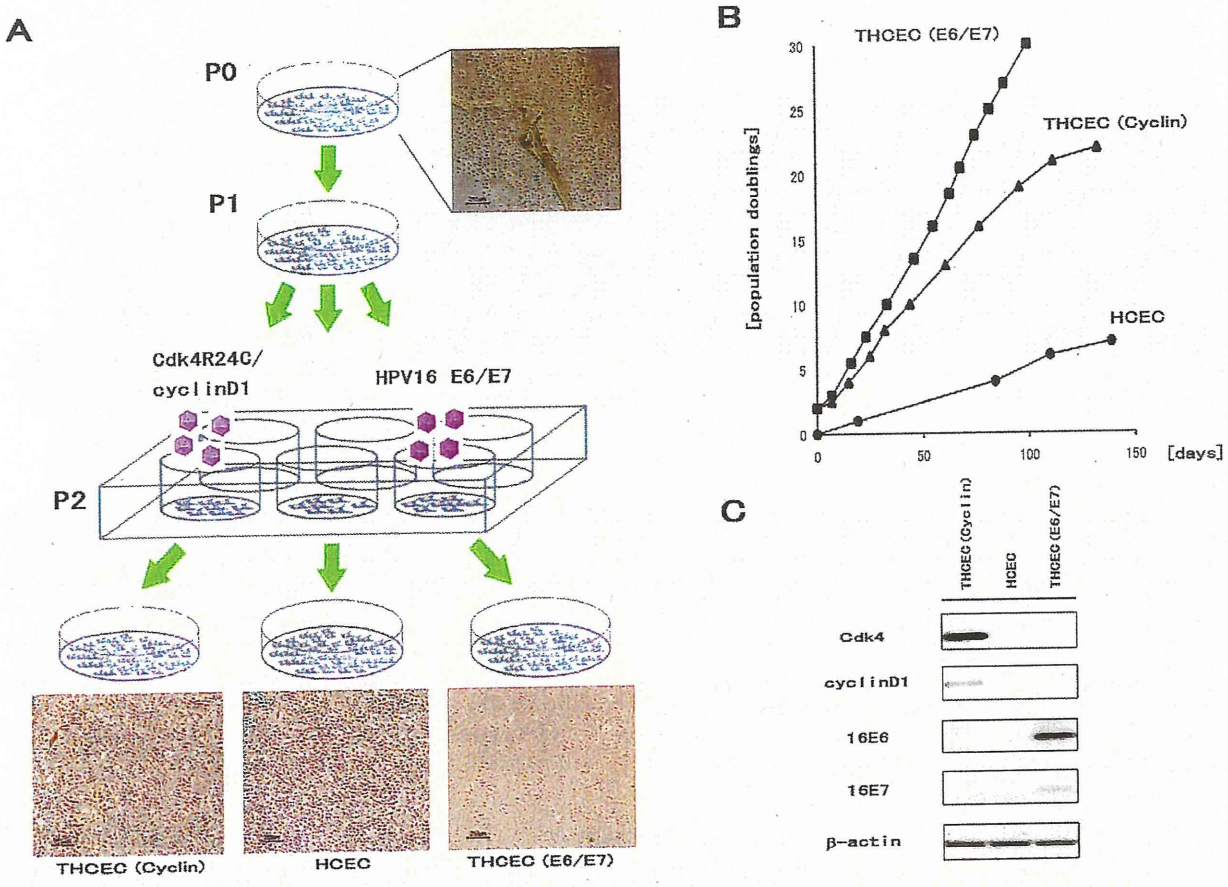

Figure 1. Establishment of THCEC (E6/E7), THCEC (Cyclin) and HCEC. (A) HCEC with Descemet's membrane were placed on Type IV collagen-coated 35 mm cell culture dishes with growth medium (P0). After one passage (P1), retroviral infection was conducted in 6-well cell culture dishes at P2. THCEC (E6/E7) and THCEC (Cyclin) were infected by retroviral vectors carrying HPV16 E6/E7 and both CyclinD1 and Cdk4R24C, respectively. (B) Growth curves of THCEC (E6/E7), THCEC (Cyclin) and HCEC cell lines. THCEC (E6/E7) was immortalized as reported previously, and THCEC (Cyclin) obtained the same proliferative activity as that of THCEC (E6/E7). Transfection was performed on day 0 for THCEC (E6/E7) and THCEC (Cyclin), with population doublings of 2. For HCEC, primary culture commenced on day 0. (C) Western blotting confirmed the expression of the following transgenes: E6 and E7 in THCEC (E6/E7), and CyclinD1 and Cdk4R24C in THCEC (Cyclin).
doi:10.1371/journal.pone.0029677.g001

morphology and physiologic function in HCEC, we only transduced mutant Cdk 4 and CyclinD1, not hTERT, in the present study. We believe that our careful method enabled THCEC (Cyclin) to form a fragile and regularly arranged monolayer complete with physiologic function.

Although THCEC (Cyclin) has similar characteristics to primary HCEC, immunohistochemistry and the Ussing chamber assay also highlighted the differences between the cells. ZO-1 protein was expressed around the nucleus of THCEC (Cyclin) but not in primary cells. Since semi-quantitative PCR detected almost the same level of mRNA expression between the cell lines, staining around the nucleus in THCEC (Cyclin) probably reflects an error in posttranslational import of ZO-1 protein. The Ussing chamber assay detected a similar pump function between THCEC (Cyclin) and primary cells, but the current in THCEC (Cyclin) was more variable than that of the primary cells, which might have been caused by reduced Na^+/K^+-ATPase activity, immature intercellular adhesion allowing irregular intercellular ion transport or differences in cellular density.

Cells established by a retrovirus carry a potential risk of promoting carcinogenesis [30], and direct transplantation to humans of cell sheets composed of such cells may lead to complex problems. Recently, to resolve this problem, several studies have reported the establishment of untransfected corneal endothelial cell lines [31,32,33], which are the most ideal cell lines for the treatment of human corneal disease. Meanwhile, alternative bioengineering approaches, including lipofection of p27kip1 siRNA [34], proteomics technology analyzing the difference between younger and older HCEC [35] and drug usage of promyelocytic leukemia zinc finger protein, a cell cycle transcriptional repressor and negative regulator [36], have also been introduced. The present findings support the idea that targeting the interaction between p16INK4a and Cdk4 using such methods is a promising strategy to generate HCEC with sufficient proliferative capacity and physiologic function.

Materials and Methods

Isolation and cell culture of human corneal cells

Ethics Statement. A cornea was excised from the surgically enucleated eye of a 2-year-old infant undergoing therapy for retinoblastoma, with the approval (approval number, #156) of the

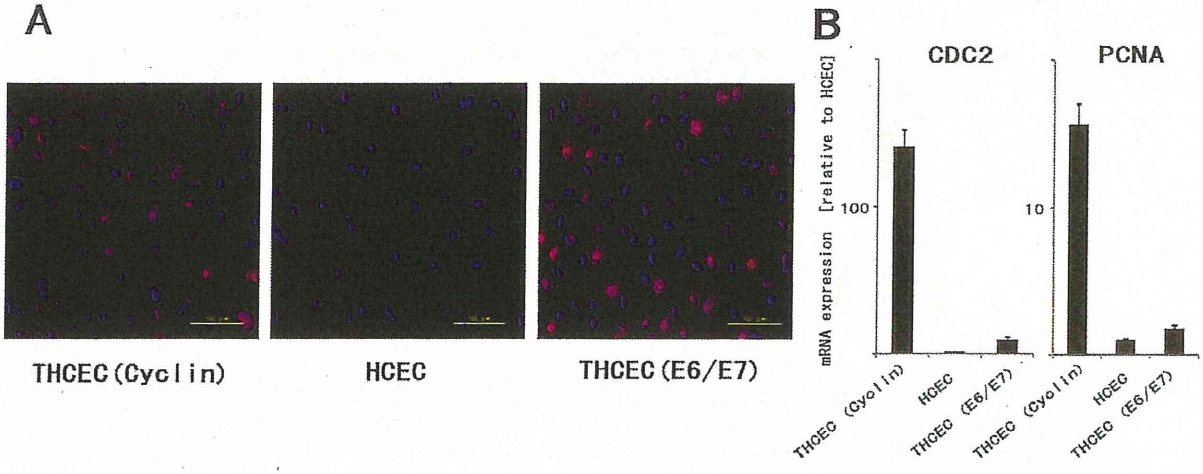

Figure 2. Evaluation of proliferative capacity. (A) Immunohistochemistry of Ki-67 in three cell lines. Positive staining of Ki-67, located in the nucleus, was obviously identified in THCEC (Cyclin) and THCEC (E6/E7), but rarely detected in HCEC. (B) Real-time PCR of downstream genes of cyclinD1 associated with proliferation. Gene expression levels of both CDC2 and PCAN were clearly higher than that of HCEC. The gene expression was much more activated in THCEC (Cyclin) in which the expression of E2F, an upstream transcriptional factor of two genes, was constitutively activated by transduced mutant Cdk4 and CyclinD1.
doi:10.1371/journal.pone.0029677.g002

Ethics Committee of the National Institute for Child and Health Development, Tokyo, Japan. Signed informed consent was obtained from the donor's parents, and the surgical specimens were irreversibly de-identified. All experiments handling human cells and tissues were performed in line with the tenets of the Declaration of Helsinki.

The corneal piece, which was grossly normal with no pathological lesions, was cut 1.5 mm from the corneal limbus,

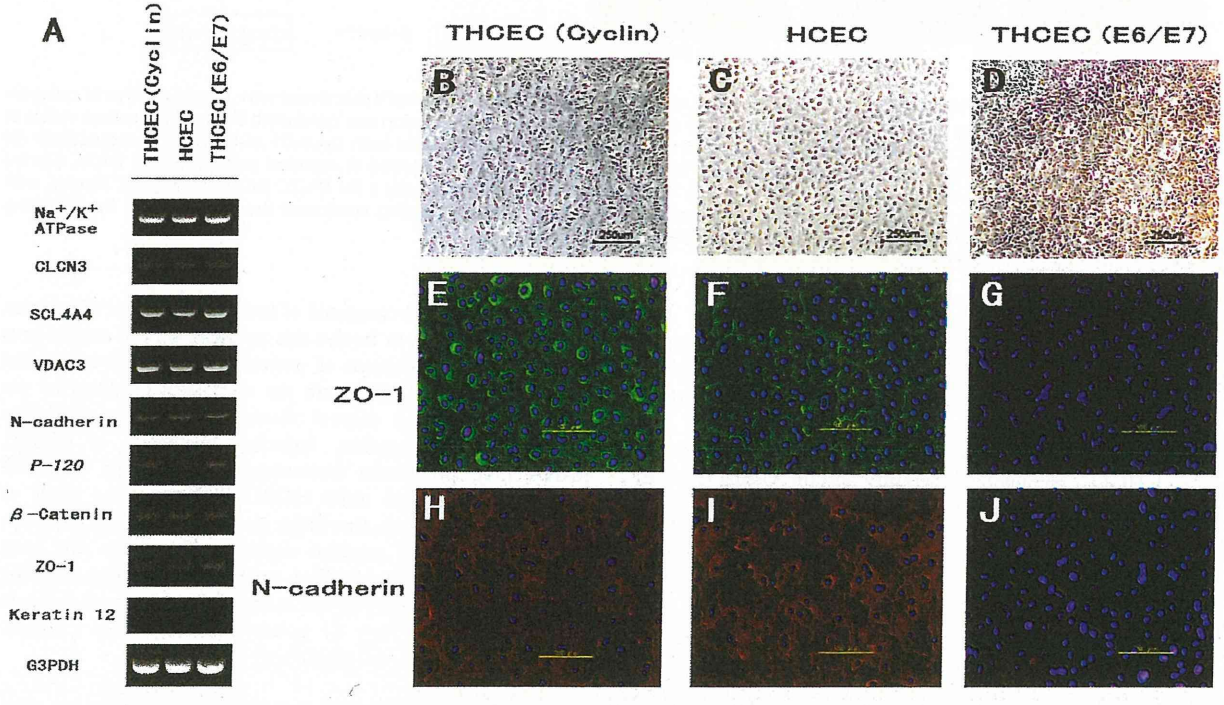

Figure 3. HCEC-associated genes and cytolocalization of junctional components expressed by cell lines. (A) Semi-quantitative reverse transcriptase polymerase chain reaction for HCEC-associated genes. Total RNA was prepared from cultured cells seven days after reaching confluency. No significant difference in mRNA expression was observed between the three cell lines. Compared with phase-contrast micrographs of (B) THCEC (Cyclin), (C) HCEC and (D) THCEC (E6/E7), cytolocalization was examined by immunofluorescence staining of ZO-1 (E, F,G) and N-cadherin (H, I, J). THCEC (E6/E7) did not stain positive for intercellular junctional molecules, while ZO-1 and N-cadherin stained positive at the junction in THCEC (Cyclin) and HCEC.
doi:10.1371/journal.pone.0029677.g003

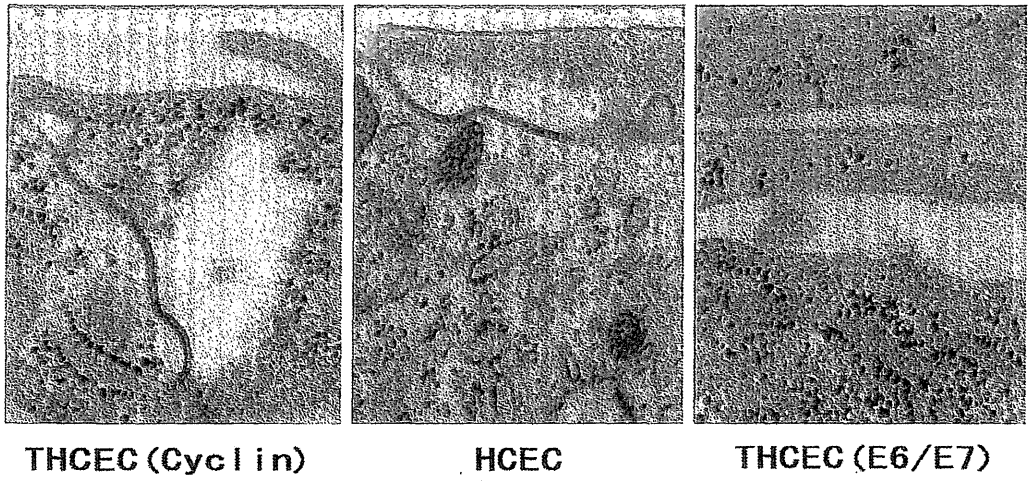

Figure 4. Transmission electron microscopy of cell line intercellular junctions. The junctional complex was detected at the intercellular junction in THCEC (Cyclin) and HCEC. No component of the intercellular junction was found in THCEC (E6/E7), in which cells grew in multilayers without being inhibited by cellular contact (scale bar = 200 nm).
doi:10.1371/journal.pone.0029677.g004

avoiding contamination of the trabecular meshwork tissue. HCEC with Descemet's membrane were stripped from the posterior surface of the corneal tissue with sterile surgical forceps under a dissecting microscope. They were cut into two pieces and cultured in a cell culture dish covered with Type IV collagen in a growth medium (GM); Dulbecco's modified Eagle's medium (DMEM)/ Nutrient mixture F12 (1:1) with high glucose supplemented with 10% fetal bovine serum, insulin-transferrin-selenium and MEM-NEAA (Gibco, Auckland, NZ). Cells were subcultured after reaching confluency by treating with trypsin/EDTA and seeded at a density of 5×10^5 cells/well in 6-well dishes.

Viral vector construction and viral transduction

Lentiviral vector plasmids, CSII-CMV-cyclin D1 and -CDK4R24C were constructed by recombination using the Gateway system (Invitrogen, Carlsbad, CA) as described previously [37]. Briefly, cDNAs of human cyclinD1 and a mutant form of Cdk4 (Cdk4R24C: an inhibitor resistant form of Cdk4, generously provided by Dr Hara) were recombined with a lentiviral vector, CSII-CMV-RfA (a gift from Dr Miyoshi), by LR reaction to create a Gateway expression plasmid (Invitrogen) according to the manufacturer's instructions.

Previous work has described the production of recombinant lentiviruses with the vesicular stomatitis virus G glycoprotein [37], the recombinant retrovirus vector plasmid, pCLXSN-16E6E7 encoding HPV16 E6/E7 (16E6E7) [38] and recombinant retroviruses [39]. Following the addition of recombinant viral fluid to cells seeded in 24-well dishes in the presence of 4 μg/ml polybrene, the cells were infected by the viruses. Stably transduced cells with an expanded life span were designated transduced

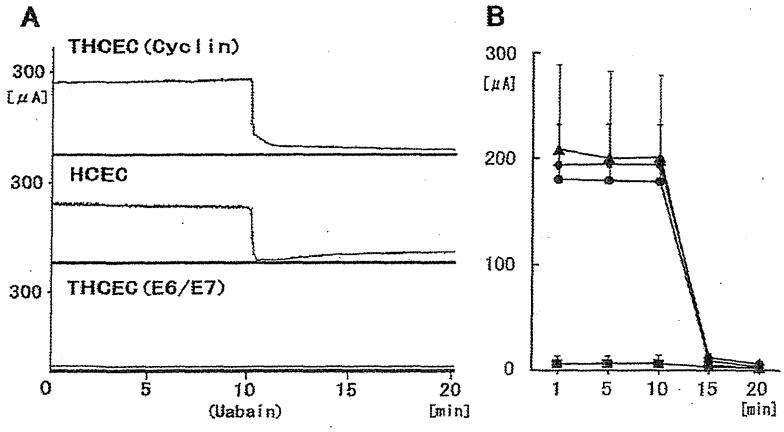

Figure 5. The pump function of cell lines. Short-circuit currents representing Na^+/K^+-ATPase activity from corneal cell monolayers on the insert well area of 4.67 cm^2 were calculated before and after addition of the Na^+/K^+-ATPase inhibitor ouabain. (A) Representative tracings of short-circuit current (μA/well) obtained with cell monolayers of THCEC (Cyclin) (upper panel), HCEC (middle panel) and THCEC (E6/E7) (lower panel). THCEC (Cyclin) possessed equal transport activity to HCEC, whereas no pump function was detected in THCEC (E6/E7). (B) Time-course changes in the average short circuit current of cultured monolayers of cell lines at 1, 5, 10 and 20 min. Data shown are for (▲) THCEC (Cyclin) at PD8, (♦) THCEC (Cyclin) at PD 21, (•) HCEC and (■) THCEC (E6/E7); all data are expressed as mean±SD of four replicate experiments of each cell line.
doi:10.1371/journal.pone.0029677.g005

Table 1. Tumorigenesis assay of cell lines in BALB/C nude mice.

Inoculated cells	Total dose (cell/mouse)	Number of mice (% mortality)	Number of mice with tumor
THCEC (Cyclin)	1.7×10^6	3(0)	0
THCEC (E6/E7)	1.7×10^6	3(0)	0
HeLa cells	2.0×10^6	3(0)	3

doi:10.1371/journal.pone.0029677.t001

human corneal endothelial cell by E6/E7 (THCEC (E6/E7)) and transduced human corneal endothelial cell by Cdk4R24C/cyclinD1 (THCEH (Cyclin)).

Culture of transfected cell lines and growth curve

When the cultures reached subconfluence, the cells were harvested with 0.25% trypsin and 1 mM EDTA, collected into tubes, and centrifuged. The cells were counted using a cell viability analyzer (Vi-CELL Cell Viability Analyzer, Beckman Coulter, Brea, CA), and population doubling (PD) was calculated. The pellets were suspended in growth medium, and the cells were passaged at a density of 5×10^5 cells/well in a 100-mm dish. The original cells were regarded as PD 2 (day 0).

Western blot analysis

Western blotting was conducted as described previously [40]. Antibodies against Cdk4 (ser473; Cell Signaling Technology, Danvers, MA), CyclinD1 (clone G124-326; BD Biosciences, Franklin Lakes, NJ), β-actin (sc-1616; Santa Cruz Biotechnology, Santa Cruz, CA) were used as probes, and horseradish peroxidase-conjugated anti-mouse, anti-rabbit (Jackson Immunoresearch Laboratories, West Grove, PA) or anti-goat (sc-2033; Santa Cruz Biotechnology, Santa Cruz, CA) immunoglobulins were employed as secondary antibodies.

Immunocytochemistry

Cell lines were grown on Type IV collagen-coated glass dishes 14 days after reaching confluency and were fixed with 4% formaldehyde (pH 7.0) for 15 min at room temperature. Cell lines were then rehydrated in phosphate buffered saline (PBS), incubated with 0.2% Triton X-100 for 15 min and rinsed three times with PBS for 5 min each. After incubation with 2% BSA to block nonspecific staining for 30 min, cell lines were incubated with anti-ZO-1 (1:50; sc-8146; Santa Cruz Biotechnology, Santa Cruz, CA), anti-N-cadherin (1:50; sc-7939; Santa Cruz Biotechnology) and anti-Ki67 (1:100; ab15580; Abcam, Cambridge, UK) for 16 h at 4°C. After three washes with PBS, cell lines were incubated with the secondary antibody for 60 min, followed by counterstaining with 4′,6-diamidino-2-phenylindole (1:200; sc-3598; Santa Cruz Biotechnology) for 10 min.

Semi-quantitative RT-PCR

Total RNA was extracted from 1×10^6 cultured HCEC using the RNeasy Plus mini-kitH (Qiagen, Germantown/Gaithersburg, MA) according to the manufacturer's instructions and quantified by absorption at 260 nm. Total RNA was then reverse-transcribed into cDNA using Superscript III Reverse Transcriptase (Invitrogen, Carlsbad, CA) with oligo random hexamers. cDNAs of each component were amplified by PCR using specific primers and DNA polymerase. The reaction was first incubated at 95°C for 10 min, followed by 39 cycles at 98°C for 30 s, 58°C for 30 s and 74°C for 30 s. PCR primers are listed in Table 2.

Quantitative real-time RT-PCR

Total RNA extraction and reverse transcription into cDNA was carried out as above. Each quantitative real-time RT-PCR for target genes, including Cell Division Cycle 2 (*CDC2*) and proliferating cell nuclear antigen (*PCNA*), was performed using the Chromo4 real time detection system (Bio-Rad, Hercules, CA). For a 20 ml PCR, the cDNA template was mixed with the primers to final concentrations of 200 nM and 10 µl of SsoFast EvaGreen Supermix (BIO-RAD), respectively. The reaction was first incubated at 95°C for 10 min, followed by 45 cycles at 95°C for 10 s, 57°C for 15 s, and 72°C for 20 s.

Transmission Electron Microscopy

Cell lines cultured on Type IV collagen-coated dishes were fixed in HEPES buffered 2% glutaraldehyde and subsequently post-fixed in 2% osmium tetroxide for 3 h on ice. Specimens were then dehydrated in graded ethanol and embedded in the epoxy resin. Ultrathin sections were obtained by ultramicrotomy and stained with uranyl acetate for 10 min and modified Sato's lead solution for 5 min then submitted to TEM observation (JEM-2000EX, JEOL).

Measurement of pump function

The pump function of confluent monolayers of HCEC was measured using an Ussing chamber as described previously [41]. Cells cultured on Snapwell inserts coated with Type IV collagen were placed in the Ussing chamber EM-CSYS-2 (Physiologic Instruments, San Diego, CA) with the endothelial cell surface side in contact with one chamber and the Snapwell membrane side in contact with another chamber. The chambers were carefully filled with Krebs-Ringer bicarbonate (120.7 mM NaCl, 24 mM $NaHCO_3$, 4.6 mM KCl, 0.5 mM $MgCl_2$, 0.7 mM Na_2HPO_4, 1.5 mM NaH_2PO_4 and 10 mM glucose bubbled with a mixture of 5% CO_2, 7% O_2 and 88% N_2 to pH 7.4). The chambers were maintained at 37°C using an attached heater.

The short-circuit current was sensed by narrow polyethylene tubes positioned close to either side of the Snapwell, filled with 3 M KCl and 4% agar gel and connected to silver electrodes. These electrodes were connected to the computer through the Ussing system VCC-MC2 (Physiologic Instruments) and an iWorx 118 Research Grade Recorder (iWorx Systems, Dover, NH), and the short-circuit current was recorded by Labscribe2 Software for Research (iWorx). After the short-circuit current had reached a steady state, ouabain (final concentration, 1 mM) was added to the chamber, and the short-circuit current was re-measured. The pump function attributable to Na^+/K^+-ATPase activity was calculated as the difference in short-circuit current measured before and after the addition of ouabain.

Tumorigenesis assay

Cells were harvested by Trypsin/EDTA treatment, collected into tubes, and centrifuged, and the pellets were suspended in

Table 2. Oligonucleotide sequences for RT-PCR.

Name	Sequence	Size (bp)	Accession Number
Collagen type IV	F: 5′-GGC ACC TGC CAC TAC TAC GC-3′	472	NM_001845
	R: 5′-TCA CCA GGA GGT AGC CGA T-3′		
Keratin 12	F: 5′-GAT GCT AAT GCT GAG CTC GA-3′	393	NM_000223
	R: 5′-ACC TGC CCT ACA GCT TTG TA-3		
VDAC3	F: 5′-TGA CTC TTG ATA CCA TAT TTG TAC CG-3′	482	NM_001135694
	R: 5′-TCA ATT TGA CTC CTG GTC GAA-3′		
CLCN3	F: 5′-AGA AAG GCA TAG ACG GAT CAA-3′	204	NM_001829
	R: 5′-GGT TGT ACC ACA ACG CAC TAA-3′		
SLC4A4	F: 5′-GTT CAG ATG AAT GGG GAT ACGC	697	NM_001136260
	R: 5′-CGA GCA TAA ACA CAA AGC GTA A-3′		
Na^+/K^+-ATPase	F: 5′-CCC AGG ACT CAT GGT TTT TC-3′	482	NM_000702
	R: 5′-GGA GCA AAG CTG ACC TGA AC-3′		
N-cadherin	F: 5′-CAA CTT GCC AGA AAA CTC CAG G-3′	205	NM_ 001792
	R: 5′-ATG AAA CCG GGC TAT CTG CTC-3′		
β-catenin	F: 5′-TAC CTC CCA AGT CCT GTA TGA G-3′	180	NM _001904
	R: 5′-TGA GCA GCA TCA AAC TGT GTA G-3′		
P-120	F: 5′-CCC CAG GAT CAC AGT CAC CT-3′	144	NM_001085467
	R: 5′-CCG AGT GGT CCC ATC ATC TG-3′		
ZO-1	F: 5′-AGT CCC TTA CCT TTC GCC TGA-3′	180	NM_003257
	R: 5′-TCT CTT AGC ATT ATG TGA GCT GC-3′		
GAPDH	F: 5′-GCT CAG ACA CCA TGG GGA AGG T-3′	474	NM_002046
	R: 5′-GTG GTG CAG GAG GCA TTG CTG A-3′		
PCNA	F: 5′- GCGTGAACCTCACCAGTATGT-3′	76	NM_002592
	R: 5′- TCTTCGGCCCTTAGTGTAATGAT-3′		
CDC2	F: 5′- GGATGTGCTTATGCAGGATTCC-3′	100	NM_001786
	R: 5′- CATGTACTGACCAGGAGGGATAG-3′		

VDAC3: voltage-dependent anion channel 3, CLCN3: chloride channel protein 3, SLC4A4: sodium bicarbonate cotransporter membrane.
doi:10.1371/journal.pone.0029677.t002

DMEM. The same volume of Basement Membrane Matrix (BD Biosciences) was added to the cell suspension. Cells (1.7×10^6) of THCEC (Cyclin) and THCEC (E6/E7) were inoculated subcutaneously into dorsal flanks of each of three Balb/c nu/nu mice (CREA, Japan) for 60 days. A total of 2.0×10^6 HeLa cells per mouse were used as positive controls. The skin of dorsal flanks of inoculated mice was surgically opened and the tumorigenic status was examined.

Author Contributions

Conceived and designed the experiments: Tadashi Yokoi YS Tae Yokoi TK AU HN NA. Performed the experiments: Tadashi Yokoi YS Tae Yokoi HM SH MY TK HN NA. Analyzed the data: Tadashi Yokoi YS Tae Yokoi HM SH MY AU HN NA. Contributed reagents/materials/analysis tools: Tadashi Yokoi SH MY TK HN NA. Wrote the paper: Tadashi Yokoi YS TK AU HN NA.

References

1. Hatou S, Yamada M, Mochizuki H, Shiraishi A, Joko T, et al. (2009) The effects of dexamethasone on the Na,K-ATPase activity and pump function of corneal endothelial cells. Curr Eye Res 34: 347–354.
2. Barfort P, Maurice D (1974) Electrical potential and fluid transport across the corneal endothelium. Exp Eye Res 19: 11–19.
3. Bourne WM, Nelson LR, Hodge DO (1997) Central corneal endothelial cell changes over a ten-year period. Invest Ophthalmol Vis Sci 38: 779–782.
4. Hashemian MN, Moghimi S, Fard MA, Fallah MR, Mansouri MR (2006) Corneal endothelial cell density and morphology in normal Iranian eyes. BMC Ophthalmol 6: 9.
5. Padilla MD, Sibayan SA, Gonzales CS (2004) Corneal endothelial cell density and morphology in normal Filipino eyes. Cornea 23: 129–135.
6. Adamis AP, Filatov V, Tripathi BJ, Tripathi RC (1993) Fuchs' endothelial dystrophy of the cornea. Surv Ophthalmol 38: 149–168.
7. Schultz RO, Matsuda M, Yee RW, Edelhauser HF, Schultz KJ (1984) Corneal endothelial changes in type I and type II diabetes mellitus. Am J Ophthalmol 98: 401–410.
8. Slingsby JG, Forstot SL (1981) Effect of blunt trauma on the corneal endothelium. Arch Ophthalmol 99: 1041–1043.
9. Bourne WM, Nelson LR, Hodge DO (1994) Continued endothelial cell loss ten years after lens implantation. Ophthalmology 101: 1014–1022;discussion 1022–1013.
10. Gagnon MM, Boisjoly HM, Brunette I, Charest M, Amyot M (1997) Corneal endothelial cell density in glaucoma. Cornea 16: 314–318.
11. Laing RA, Sanstrom MM, Berrospi AR, Leibowitz HM (1976) Changes in the corneal endothelium as a function of age. Exp Eye Res 22: 587–594.
12. Landshman N, Ben-Hanan I, Assia E, Ben-Chaim O, Belkin M (1988) Relationship between morphology and functional ability of regenerated corneal endothelium. Invest Ophthalmol Vis Sci 29: 1100–1109.
13. Coster DJ, Williams KA (2005) The impact of corneal allograft rejection on the long-term outcome of corneal transplantation. Am J Ophthalmol 140: 1112–1122.
14. Terry MA, Ousley PJ (2001) Deep lamellar endothelial keratoplasty in the first United States patients: early clinical results. Cornea 20: 239–243.
15. Price FW Jr., Price MO (2005) Descemet's stripping with endothelial keratoplasty in 50 eyes: a refractive neutral corneal transplant. J Refract Surg 21: 339–345.
16. Melles GR, Ong TS, Ververs B, van der Wees J (2006) Descemet membrane endothelial keratoplasty (DMEK). Cornea 25: 987–990.

17. Zhu C, Joyce NC (2004) Proliferative response of corneal endothelial cells from young and older donors. Invest Ophthalmol Vis Sci 45: 1743–1751.
18. Li W, Sabater AL, Chen YT, Hayashida Y, Chen SY, et al. (2007) A novel method of isolation, preservation, and expansion of human corneal endothelial cells. Invest Ophthalmol Vis Sci 48: 614–620.
19. Ishino Y, Zhu C, Harris DL, Joyce NC (2008) Protein tyrosine phosphatase-1B (PTP1B) helps regulate EGF-induced stimulation of S-phase entry in human corneal endothelial cells. Mol Vis 14: 61–70.
20. Senoo T, Joyce NC (2000) Cell cycle kinetics in corneal endothelium from old and young donors. Invest Ophthalmol Vis Sci 41: 660–667.
21. Kim HJ, Ryu YH, Ahn JI, Park JK, Kim JC (2006) Characterization of immortalized human corneal endothelial cell line using HPV 16 E6/E7 on lyophilized human amniotic membrane. Korean J Ophthalmol 20: 47–54.
22. Nitta M, Katabuchi H, Ohtake H, Tashiro H, Yamaizumi M, et al. (2001) Characterization and tumorigenicity of human ovarian surface epithelial cells immortalized by SV40 large T antigen. Gynecol Oncol 81: 10–17.
23. Tsao SW, Mok SC, Fey EG, Fletcher JA, Wan TS, et al. (1995) Characterization of human ovarian surface epithelial cells immortalized by human papilloma viral oncogenes (HPV-E6E7 ORFs). Exp Cell Res 218: 499–507.
24. Zhu YT, Hayashida Y, Kheirkhah A, He H, Chen SY, et al. (2008) Characterization and comparison of intercellular adherent junctions expressed by human corneal endothelial cells in vivo and in vitro. Invest Ophthalmol Vis Sci 49: 3879–3886.
25. Kiyono T, Foster SA, Koop JI, McDougall JK, Galloway DA, et al. (1998) Both Rb/p16INK4a inactivation and telomerase activity are required to immortalize human epithelial cells. Nature 396: 84–88.
26. Sekiguchi T, Hunter T (1998) Induction of growth arrest and cell death by overexpression of the cyclin-Cdk inhibitor p21 in hamster BHK21 cells. Oncogene 16: 369–380.
27. Sasaki R, Narisawa-Saito M, Yugawa T, Fujita M, Tashiro H, et al. (2009) Oncogenic transformation of human ovarian surface epithelial cells with defined cellular oncogenes. Carcinogenesis 30: 423–431.
28. Rane SG, Cosenza SC, Mettus RV, Reddy EP (2002) Germ line transmission of the Cdk4(R24C) mutation facilitates tumorigenesis and escape from cellular senescence. Mol Cell Biol 22: 644–656.
29. Enomoto K, Mimura T, Harris DL, Joyce NC (2006) Age differences in cyclin-dependent kinase inhibitor expression and rb hyperphosphorylation in human corneal endothelial cells. Invest Ophthalmol Vis Sci 47: 4330–4340.
30. Robinson HL (1982) Retroviruses and cancer. Rev Infect Dis 4: 1015–1025.
31. Fan T, Zhao J, Ma X, Xu X, Zhao W, et al. (2011) Establishment of a continuous untransfected human corneal endothelial cell line and its biocompatibility to denuded amniotic membrane. Mol Vis 17: 469–480.
32. Fan T, Wang D, Zhao J, Wang J, Fu Y, et al. (2009) Establishment and characterization of a novel untransfected corneal endothelial cell line from New Zealand white rabbits. Mol Vis 15: 1070–1078.
33. Valtink M, Gruschwitz R, Funk RH, Engelmann K (2008) Two clonal cell lines of immortalized human corneal endothelial cells show either differentiated or precursor cell characteristics. Cells Tissues Organs 187: 286–294.
34. Kikuchi M, Zhu C, Senoo T, Obara Y, Joyce NC (2006) p27kip1 siRNA induces proliferation in corneal endothelial cells from young but not older donors. Invest Ophthalmol Vis Sci 47: 4803–4809.
35. Zhu C, Rawe I, Joyce NC (2008) Differential protein expression in human corneal endothelial cells cultured from young and older donors. Mol Vis 14: 1805–1814.
36. Shiraishi A, Joko T, Higashiyama S, Ohashi Y (2007) Role of promyelocytic leukemia zinc finger protein in proliferation of cultured human corneal endothelial cells. Cornea 26: S55–58.
37. Miyoshi H, Blomer U, Takahashi M, Gage FH, Verma IM (1998) Development of a self-inactivating lentivirus vector. J Virol 72: 8150–8157.
38. Narisawa-Saito M, Yoshimatsu Y, Ohno S, Yugawa T, Egawa N, et al. (2008) An in vitro multistep carcinogenesis model for human cervical cancer. Cancer Res 68: 5699–5705.
39. Naviaux RK, Costanzi E, Haas M, Verma IM (1996) The pCL vector system: rapid production of helper-free, high-titer, recombinant retroviruses. J Virol 70: 5701–5705.
40. Haga K, Ohno S, Yugawa T, Narisawa-Saito M, Fujita M, et al. (2007) Efficient immortalization of primary human cells by p16INK4a-specific short hairpin RNA or Bmi-1, combined with introduction of hTERT. Cancer Sci 98: 147–154.
41. Mimura T, Yamagami S, Yokoo S, Usui T, Tanaka K, et al. (2004) Cultured human corneal endothelial cell transplantation with a collagen sheet in a rabbit model. Invest Ophthalmol Vis Sci 45: 2992–2997.

Carcinogenesis Advance Access published March 1, 2012
Carcinogenesis vol.0 no.0 pp.1–8, 2012
doi:10.1093/carcin/bgs104
Advance Access publication February 15, 2012

A critical role of MYC for transformation of human cells by HPV16 E6E7 and oncogenic HRAS

Mako Narisawa-Saito[1,†], Yuki Inagawa[1,†], Yuki Yoshimatsu[1], Kei haga[1], Katsuyuki Tanaka[1], Nagayasu Egawa[1], Shin-ichi Ohno[1], Hitoshi Ichikawa[2], Takashi Yugawa[1], Masatoshi Fujita[1,3] and Tohru Kiyono[1,*]

[1]Division of Virology and [2]Division of Genetics, National Cancer Center Research Institute, 5-1-1 Tsukiji, Chuo-ku, Tokyo 104-0045, Japan and [3]Department of Cellular Biochemistry, Graduate School of Pharmaceutical Sciences, Kyushu University, 3-1-1 Maidashi, Higashi-ku, Fukuoka 812-8582, Japan

*To whom correspondence should be addressed. Tel: +81 3 3547 5275; Fax: +81 3 3543 2181; Email: tkiyono@ncc.go.jp

Human papillomaviruses (HPVs) are the primary causal agents for development of cervical cancer, and deregulated expression of two viral oncogenes E6 and E7 is considered to contribute to disease initiation. Recently, we have demonstrated that transduction of oncogenic HRAS ($HRAS^{G12V}$) and MYC together with HPV16 E6E7 is sufficient for tumorigenic transformation of normal human cervical keratinocytes (HCKs). Here, we show that transduction of $HRAS^{G12V}$ on the background of E6E7 expression causes accumulation of MYC protein and tumorigenic transformation of not only normal HCKs but also other normal primary human cells, including tongue keratinocytes and bronchial epithelial cells as well as hTERT-immortalized foreskin fibroblasts. Subcutaneous transplantation of as few as 200 HCKs expressing E6E7 and $HRAS^{G12V}$ resulted in tumor formation within 2 months. Dissecting RAS signaling pathways, constitutively active forms of AKT1 or MEK1 did not result in tumor formation with E6E7, but tumorigenic transformation was induced with addition of MYC. Increased MYC expression endowed resistance to calcium- and serum-induced terminal differentiation and activated the mammalian target of rapamycin (mTOR) pathway. An mTOR inhibitor (Rapamycin) and MYC inhibition a level not affecting proliferation in culture both markedly suppressed tumor formation by HCKs expressing E6E7 and $HRAS^{G12V}$. These results suggest that a single mutation of HRAS could be oncogenic in the background of deregulated expression of E6E7 and MYC plays a critical role in cooperation with the RAS signaling pathways in tumorigenesis. Thus inhibition of MYC and/or the downstream mTOR pathway could be a therapeutic strategy not only for the MYC-altered but also RAS-activated cancers.

Introduction

A subset of human papillomaviruses (HPVs), the so called high-risk types such as type 16 and 18, are associated with >90% of all cervical carcinomas as primary causal agents (1), with deregulated expression of the HPV viral oncogenes E6 and E7 as the main contributors to an etiology (2). However, epidemiological studies and experimental data indicate that the viral presence is not enough to induce cervical cancer and additional genetic and epigenetic events (to alter the cellular factors) are presumably required (3). To address this, we have established an *in vitro* model for cervical cancer with normal human cervical keratinocytes (HCKs) focusing on sequential transduction of defined genetic elements (4) and succeeded in the creation of highly potent cancer initiating cells by introduction of c-MYC (MYC) and oncogenic $HRAS^{G12V}$ (HRAS) on a background of HPV16 E6 and E7 expression (4). However, since the cells having been cultivated in the differentiating medium were used for the assays, we could not exclude the possibility that genetic and/or epigenetic alterations during the selection might be critical for the transformation. In the present study, by directly examining transformed phenotype of the cells without such selection, we could demonstrate that oncogenic HRAS, without overexpression of exogenous MYC, is sufficient for tumorigenic transformation of normal human cells expressing E6 and E7. Nonetheless, endogenous MYC stabilized by HRAS was revealed to be a critical player in tumor-initiating potential.

Abbreviations: DMEM, Dulbecco's modified Eagle's medium; ERK, extracellular signal-regulated kinase; ES, embryonic stem cell; HBEC, human bronchial epithelial cell; HCK, human cervical keratinocyte; HFF, human foreskin fibroblast; HPV, human papillomavirus; KGM, keratinocyte growth medium; mTOR, mammalian target of rapamycin.

†These authors contributed equally to this work.

Materials and methods

Cell culture and cell lines

Normal HCKs were obtained with written consent from patients who underwent abdominal surgery for a gynecological disease other than cervical cancer. HCK1, HCK4 and HCK8 cells derived from different donors were maintained in low-calcium serum-free keratinocyte growth medium (KGM) (Epilife-KG2 KURABO Industries, Ltd, Osaka, Japan) unless otherwise described. HCK1T cells were established by transduction of *hTERT* into HCK1 cells (4). These HCK cells were then further transduced with HPV16 *E6E7* followed by the oncogene(s) of interest. Normal human bronchial epithelial cells (HBECs) were purchased from Cell Applications (San Diego) and cultivated in KGM. Normal human foreskin fibroblasts (HFFs) purchased from BioWhittaker (Walkersville) were immortalized by transduction of *hTERT*. HFFs and cervical cancer cell lines, SiHa, CaSki and HeLa and C33A, were grown in Dulbecco's modified Eagle's medium (DMEM) (Sigma) containing 10% fetal bovine serum. The source, authentication and methods of maintenance of the cell lines are described in the Supplementary Materials and Methods, available at *Carcinogenesis* Online.

Vector construction and retroviral infection

Construction of the retroviral expression vectors, pCLXSN-16E6E7, pCLXSH-hTERT, pCMSCVpuro-MYC, pCLMSCV-puro-BCL2, pCMSCVpuro-myr-AKT1, pCMSCVbsd-$HRAS^{G12V}$, pCMSCVbsd and pCMSCVpuro-MEK1DD was as described previously (4,5). OmoMYC, a human version of the dominant-interfering MYC mutant (6), which encodes the C-terminal 92 amino acids of MYC with four amino acid substitutions (E410T, E417I, R423Q and R424N) and MYC^{T58A} were made by *in vitro* mutagenesis and cloned into a lentiviral vector, CSII-TRE-Tight-RfA, in which the elongation factor promoter in CSII-EF-RfA (a gift from Hiroyuki Miyoshi, RIKEN, BioResource Center) was replaced with the tetracycline-responsive promoter from pTRE-Tight (Clonetech). CSII-TRE-Tight-16E6E7-2A-MYC^{T58A}-2A-$HRAS^{G12V}$ was constructed by inserting the 16E6E7, MYC^{T58A} and $HRAS^{G12V}$ segments separated by the sequences encoding the autonomous 'self-cleaving' 2A peptides derived from foot-and-mouse disease virus (7) into CSII-TRE-Tight-RfA. CSII-TRE-Tight-MYCmiR-1, -2 and -3 were constructed by inserting the micro RNA sequence based on the BLOCK-iT Pol II miR RNAi system (Invitrogen) into CSII-TRE-Tight-RfA. The target sequence for MYCmiR-1, -2 and -3 are 5′-TAGTC-GAGGTCATAGTTCCTG-3′, 5′-ATGAAACTCTGGTTCACCATG-3′ and 5′-TTGACATTCTCCTCGGTGTCC-3′, respectively. The production of recombinant viruses and selection of infected HCKs were detailed earlier (4,5).

Western analysis

Western blotting was conducted as described previously (4). Antibodies used were listed in the Supplementary Material and Methods, available at *Carcinogenesis* Online.

Colony formation in soft agar medium

Cells were seeded at 5×10^4 cells per 35 mm dish (BD-Falcon 3046) in an appropriate medium. Colonies over 50 μm in diameter were counted after 3 weeks as described previously (4).

Clonogenic assay

Aliquots of 500 cells were seeded on 35 mm dishes under sparse conditions. After cultivation for 2 weeks, the cells were stained with Giemsa's dye, and the number of colonies was counted.

Tumorigenesis in nude mice

All surgical procedures and care administered to the animals were in accordance with institutional guidelines. A 100 µl volume of cells in a 1:1 mixture of Matrigel (BD Biosciences) was subcutaneously injected into female BALB/c nude mice (Clea Japan). The expression of human involucrin in all tumors was determined by western blots with antibodies against human involucrin that do not react with mouse epidermis to confirm that the tumors were derived from implanted HCKs (data not shown).

Quantitative reverse transcription–PCR analysis

Quantitative reverse transcription–PCR was performed as described previously (8). Amplified products were detected with a TaqMan Gene Expression Assay (Applied Biosystems). The expression level of the MYC gene was then normalized to RNA content for each sample using beta-2-microglobulin messenger RNA as a control.

Results

Oncogenic HRAS is sufficient for tumor initiation with normal human cells expressing HPV16 E6E7

Previously, we demonstrated that introduction of HPV16 *E6* and *E7* (E6E7), *H-RAS^{G12V}* (HRAS) and *c-MYC* (MYC) to normal HCKs transduced with hTERT (HCK1T) resulted in the creation of highly potent tumor-initiating cells capable of forming tumors in nude mice when only 10 cells were transplanted subcutaneously (4). Since the cells having been cultivated in the differentiating medium containing high calcium and serum (DMEM + 10% fetal bovine serum; DMEM hereafter) were used for the assays, it is possible that such adaptation or selection was required for the tumor-initiating potential by adding further epigenetic or even genetic alteration(s). To exclude the possibility, we directly examined transformed phenotype of the cells soon after transduction of oncogenes cultivated in KGM and revealed that HRAS addition was sufficient for tumorigenic transformation of primary HCKs and HCKTs (HCKT where T is for hTERT) expressing HPV16 E6E7 (Table I, A). In the presence of HRAS, endogenous MYC protein levels were markedly elevated (Figure 1A). When 1 million cells were subcutaneously transplanted into nude mice, HCK4T-E (E is for E6E7) expressing HRAS formed large tumors within 2 weeks, irrespective of the presence of an exogenous MYC transgene although growth was marginally faster with the latter (Figure 1B; $P > 0.05$). A high proportion of tumor-initiating cells in populations expressing E6E7 and HRAS was confirmed by injecting only 200 cells of different batches of HCKTs expressing the same set of genes into nude mice, resulting in tumor formation within 2 months (Table I, B). Thus, we examined whether HPV16 E6E7 and HRAS with or without exogenous MYC could confer tumor formation properties on other human cell types, including HBEC and HFF immortalized with hTERT (Figure 1D and E). Although, exogenous MYC expression resulted in the faster tumor-forming ability of HBEC ($P < 0.0005$), E6E7 and HRAS was sufficient for tumorigenic potential of these human cells with increased endogenous MYC levels (Figure 1C).

Then, we examined the effect of induced expression of MYC^{T58A}, which is a form resistant to FBWX7-dependent proteasomal degradation (9), on the tumorigenic potential of HCK1T-E with HRAS cells. Although MYC^{T58A} accumulation was observed in doxycycline-treated cells both *in vitro* and *in vivo*, it did not result in increased tumorigenic potential in this setting (Supplementary Figure 1 is available at *Carcinogenesis* Online), indicating the possibility that certain threshold levels of MYC stabilized by HRAS might be sufficient.

Table 1. Summary of xenograft transplantation of HCKs

(A) Tumor formation using E6E7 expressing HCKs with HRAS^{G12V}

Cells	No. of tumors per sites of injection 1 × 10^6 cells per site	Weight of tumors (mg) at the end of the experiment (weeks)
HCK1T	4/4	460 ± 137 (3 weeks)
HCK1Ta	4/4	640 ± 479 (2 weeks)
HCK1Tb	4/4	500 ± 338 (2 weeks)
HCK1Tc	4/4	140 ± 50 (2 weeks)
HCK4T	4/4	523 ± 148 (2 weeks)
HCK4	4/4	225 ± 50 (3 weeks)
HCK8	4/4	555 ± 140 (3 weeks)

(B) Tumor formation using E6E7 expressing HCKs with HRAS^{G12V}

	2 × 10^3 cells per site (weeks)	2 × 10^2 cells per site (weeks)
HCK1T	6/6 (4)	6/6 (4)
HCK4T	4/4 (4)	4/4 (6)
HCK8T	4/4 (4)	4/4 (6)

(C) Tumor formation using E6E7 expressing HCK1T cells with MYC or other downstream signals of HRAS^{G12V}

	No. of tumors per sites of injection (1 × 10^6 cells per site)				
HCK1T-E6E7-	vect (weeks)	MYC	MYC^{T58A}	Tet-inducible-MYC^{T58A}	
				Dox+ (weeks)	Dox− (weeks)
Vect	0/7	0/4	0/4	0/3	0/3
BCL2			1/4	1/3	0/3
AKT	0/4			3/3 (9)	3/3 (9)[a]
MEK1DD	0/4			4/4 (7)	3/3 (7)[a]
HRAS^{G12V}	12/12 (2)			10/10 (6)[b]	10/10 (6)[b]

(B) Latency was determined as the time taken before a palpable mass could be detected and indicated in parentheses (weeks). (C) Incidence of tumor formation within 20 weeks of observation period was scored otherwise observation was terminated at the time indicated in parentheses (weeks). No description indicates not determined.

[a]Only small tumors developed as in Figure 3B and C.

[b]10^3 ($n = 4$) or 10^2 ($n = 6$) cells were transplanted.